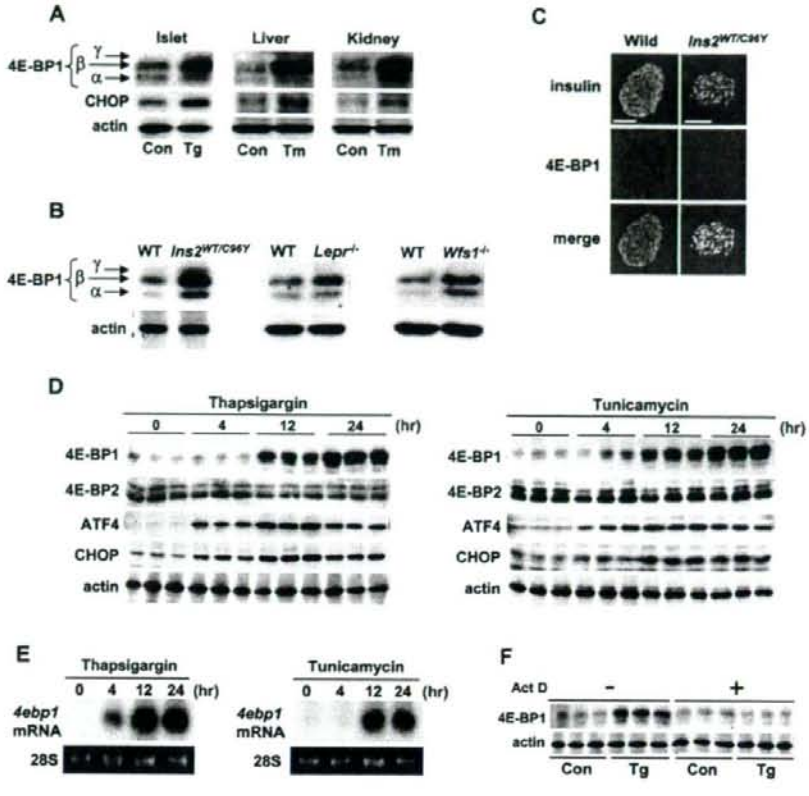

Figure 1. ER Stress Induces 4E-BP1 Expression

(A) Expression of 4E-BP1 protein in isolated islets treated with vehicle (0.05% DMSO) control (Con) or 0.5 μM thapsigargin (Tg) for 12 hr. 4E-BP1 expression was also examined in the livers and kidneys of mice that had received intraperitoneal injections of tunicamycin (Tm) 96 hr previously.

(B) Expression of 4E-BP1 protein in islets from wild-type (WT), *Ins2*$^{WT/C96Y}$, *Lepr* $^{-/-}$, and *Wfs1* $^{-/-}$ mice.

(C) Immunostaining of pancreatic sections from WT and *Ins2*$^{WT/C96Y}$ mice using anti-insulin and anti-4E-BP1 antibodies. Scale bars = 50 μm.

(D and E) Time courses of 4E-BP1, 4E-BP2, ATF4, and CHOP expression (D) and *4ebp1* mRNA expression (E) in MIN6 cells treated with thapsigargin (left panel) or tunicamycin (right).

(F) Inhibition of 4E-BP1 induction by actinomycin D (1 μg/ml) in MIN6 cells treated with thapsigargin for 12 hr.

one of three isoforms of the 4E-BP family, in β cells under ER stress.

RESULTS

ER Stress Induces 4E-BP1

4E-BP1 protein is present in three forms with different phosphorylation states. The hypophosphorylated α and β forms are active and the hyperphosphorylated γ form is inactive in terms of eIF4E binding. Expression of 4E-BP1 protein, especially the hypophosphorylated forms, was markedly induced, with an increase in CHOP, a stress marker protein, in isolated islets treated with thapsigargin (an ER Ca^{2+} pump inhibitor causing ER stress) (Figure 1A). 4E-BP1 induction was also observed in liver and kidneys of mice administered tunicamycin (a protein glycosylation inhibitor), another ER stress inducer (Figure 1A).

Furthermore, 4E-BP1 protein expression was markedly increased in *Ins2*$^{WT/C96Y}$ islets (Figures 1B and 1C), in which misfolded insulin molecules with a C96Y mutation cause ER stress (Wang et al., 1999). Islets from leptin receptor null (*Lepr* $^{-/-}$) mice, which have been shown to suffer from ER stress (Laybutt et al., 2007), also exhibited increased 4E-BP1 expression (Figure 1B). The *Wfs1* $^{-/-}$ mouse (Ishihara et al., 2004) is a model of Wolfram syndrome, which is characterized by juvenile-onset diabetes mellitus and optic atrophy and is caused by *WFS1* mutations (Inoue et al., 1998; Strom et al., 1998). WFS1-deficient islets are affected by chronic ER stress (Ishihara et al., 2004; Riggs et al., 2005). Again, 4E-BP1 protein was increased in *Wfs1* $^{-/-}$ islets (Figure 1B).

Induction of 4E-BP1 by ER stress was also observed in insulinoma MIN6 cells (Miyazaki et al., 1990) (Figure 1D). Expression of 4E-BP2, another member of the 4E-BP family, remained unchanged. While expression of ATF4 and CHOP peaked at 12 hr after treatment with thapsigargin or tunicamycin, 4E-BP1 protein was further increased at 24 hr posttreatment (Figure 1D). 4E-BP1 protein induction appeared to result from transcriptional

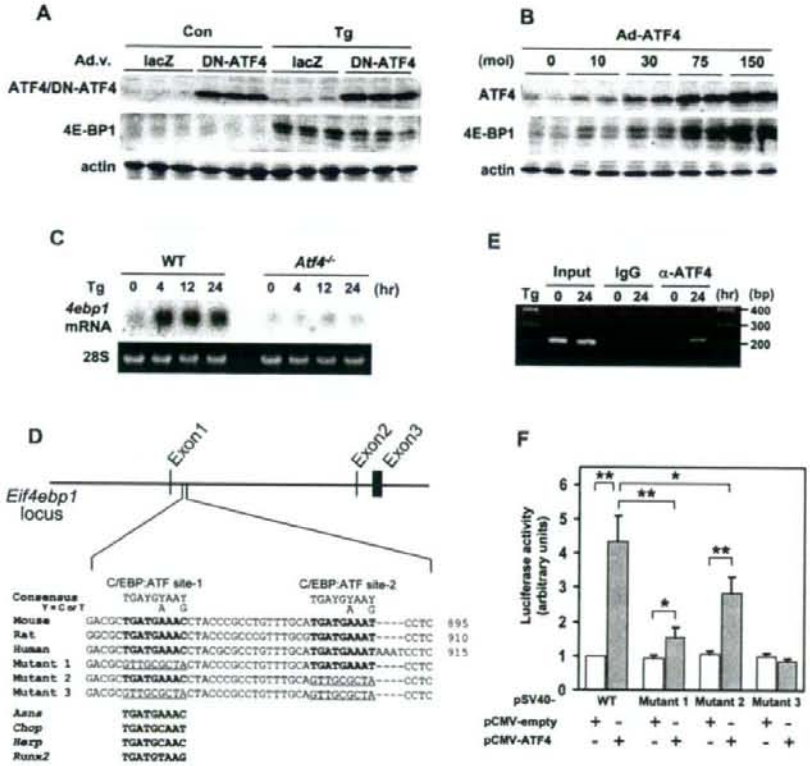

Figure 2. *Eif4ebp1* Is a Direct Target of ATF4

(A) Suppression of thapsigargin (Tg, 0.5 μM)-induced 4E-BP1 expression by dominant-negative ATF4 (DN-ATF4). MIN6 cells were infected with an adenovirus expressing either lacZ or DN-ATF4. Two days later, the cells were treated with vehicle (0.05% DMSO) control (Con) or Tg for 12 hr.

(B) 4E-BP1 expression in MIN6 cells infected with an adenovirus expressing wild-type ATF4 at the indicated multiplicity of infection (moi).

(C) *4ebp1* mRNA levels in wild-type and *Atf4*$^{-/-}$ MEFs treated with thapsigargin.

(D) C/EBP:ATF composite sites in intron 1 of the *Eif4ebp1* gene. Mouse, rat, and human *Eif4ebp1* gene segments are aligned with ATF4 binding sequences in several genes. Numbers are positions relative to A of the initial ATG codon. *Asns*, asparagine synthetase; *Herp*, homocysteine-induced ER protein; *Runx2*, runt-related transcription factor 2.

(E) Chromatin immunoprecipitation assay of MIN6 cells treated with thapsigargin. DNAs precipitated with nonspecific or anti-ATF4 IgG were amplified using primers for the *Eif4ebp1* intron 1 region.

(F) ATF4 induction of luciferase reporters with the *SV40* promoter and an *Eif4ebp1* gene segment with C/EBP:ATF composite sites or their mutants shown in (D). MIN6 cells were transfected with luciferase reporters together with either pCMV-empty or pCMV-ATF4. Error bars represent SEM. n = 4; *$p < 0.05$, **$p < 0.01$.

activation since *4ebp1* mRNA levels were also increased by these ER stress inducers (Figure 1E) and the transcriptional inhibitor actinomycin D completely blocked 4E-BP1 induction by thapsigargin (Figure 1F).

ATF4 Directly Activates the *Eif4ebp1* Gene

MIN6 cells were infected with recombinant adenoviruses expressing dominant-negative (DN) forms of transcription factors involved in the UPR. Expression of DN-ATF4 (He et al., 2001) (Figure 2A), but not DN-ATF6 or DN-XBP1 (see Figure S1 available online), suppressed 4E-BP1 induction by thapsigargin. Conversely, expression of wild-type ATF4 dramatically induced 4E-BP1 expression (Figure 2B). Furthermore, *4ebp1* mRNA levels were not increased by thapsigargin in *Atf4*$^{-/-}$ murine embryonic fibroblasts (MEFs) (Harding et al., 2003) (Figure 2C).

A survey of the mouse *Eif4ebp1* gene using a luciferase assay identified a segment in intron 1 that conferred thapsigargin sensitivity to a luciferase reporter (Figure S2). Indeed, we found two potential ATF4 binding sequences (C/EBP:ATF composite sites) in this segment (Figure 2D). Chromatin immunoprecipitation (ChIP) assays revealed that ATF4 binds this segment (Figure 2E). Furthermore, cotransfection of a luciferase reporter containing the C/EBP:ATF sites with an ATF4-expressing plasmid increased luciferase activity by 4.3-fold (Figure 2F). Disruption of the upstream C/EBP:ATF site (mutant 1) or the downstream site (mutant 2) decreased the ATF4-mediated increase in luciferase activity by 83% or 47%, respectively, and disruption of both (mutant 3) completely abolished the increase (Figure 2F).

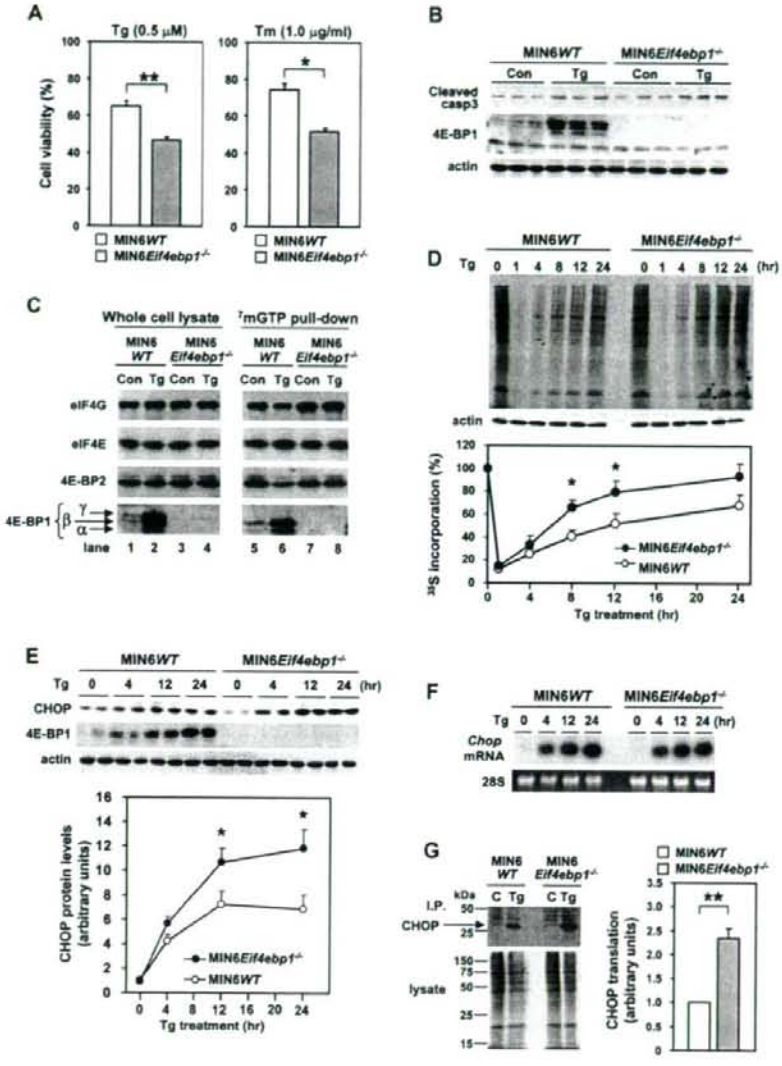

Figure 3. 4E-BP1-Deficient Cells Exhibit Increased Apoptosis Susceptibility with Deregulated Translational Control

(A) Viability of MIN6*WT* and MIN6*Eif4ebp1* $^{-/-}$ cells treated with 0.5 μM thapsigargin (Tg) or 1.0 μg/ml tunicamycin (Tm) for 36 hr, normalized to MIN6*WT* cells treated with vehicle (0.05% DMSO). n = 3–4.

(B) Immunoblot of cleaved caspase-3 in MIN6*WT* and MIN6*Eif4ebp1* $^{-/-}$ cells treated with vehicle control (Con) or thapsigargin for 24 hr.

(C) Immunoblot analysis of 4E-BP1, 4E-BP2, eIF4E, and eIF4G in whole-cell lysates (left) or in a complex associated with ^{7}mGTP-Sepharose (right) in cells treated with thapsigargin for 24 hr.

(D) [^{35}S]methionine/cysteine incorporation during a 15 min pulse labeling in MIN6*WT* and MIN6*Eif4ebp1* $^{-/-}$ cells pretreated with thapsigargin for the indicated periods. Ten percent of the lysates were also probed with an anti-actin antibody. A representative autoradiogram is shown in the upper panel; data from three experiments are summarized in the lower panel.

(E) Increased CHOP induction in MIN6*Eif4ebp1* $^{-/-}$ cells treated with thapsigargin. Representative blots are shown in the upper panel; data from four experiments are summarized in the lower panel.

(F) *Chop* mRNA levels in MIN6*WT* and MIN6*Eif4ebp1* $^{-/-}$ cells treated with thapsigargin.

(G) Greater *Chop* translation in MIN6*Eif4ebp1* $^{-/-}$ cells treated with thapsigargin. MIN6*WT* and MIN6*Eif4ebp1* $^{-/-}$ cells treated with vehicle (C) or thapsigargin (Tg) for 12 hr were labeled with [^{35}S]methionine/cysteine. Lysates were either directly subjected to SDS-PAGE or immunoprecipitated with anti-CHOP antibody. Representative autoradiograms are shown in the left panel; data from four experiments are summarized in the right panel.

Error bars represent SEM. $^{*}p < 0.05$, $^{**}p < 0.01$.

4E-BP1-Deficient β Cells Are More Vulnerable to ER Stress

A 4E-BP1-deficient β cell line, MIN6*Eif4ebp1* $^{-/-}$, was established by crossing *Eif4ebp1* $^{-/-}$ mice (Tsukiyama-Kohara et al., 2001) with IT6 mice expressing SV40 large T antigen in β cells (Miyazaki et al., 1990). MIN6 cells with wild-type *Eif4ebp1* alleles, established in parallel, were designated MIN6*WT* cells. MIN6*Eif4ebp1* $^{-/-}$ cells were more vulnerable to ER stress inducers than MIN6*WT* cells (Figure 3A). 4E-BP1 re-expression restored this diminished viability of MIN6*Eif4ebp1* $^{-/-}$ cells to control levels (Figure S3A). The increased susceptibility to ER stress-induced cell death was accompanied by enhanced caspase-3 cleavage (Figure 3B), indicating that the reduced viability of MIN6*Eif4ebp1* $^{-/-}$ cells was due at least in part to increased apoptosis. In addition, DNA fragmentation under ER stress was greater in *Eif4ebp1* $^{-/-}$ islets than in wild-type islets (Figure S3B). These results suggest that 4E-BP1 induction contributes to β cell survival under ER stress.

We then examined the impact of 4E-BP1 deficiency on the integrity of the eIF4F translational initiation complex. Pull-down assays of eIF4E and its binding partners with a cap analog, 7-methyl-GTP, revealed that thapsigargin-induced 4E-BP1 expression resulted in marked increases in the amounts of hypophosphorylated 4E-BP1 α and β forms bound to eIF4E, displacing eIF4G from eIF4E in MIN6*WT* cells (Figure 3C, compare lane 5 with lane 6). The amount of eIF4G bound to eIF4E was reduced to 63% ± 3% ($n = 4$, $p < 0.05$) of that in vehicle-treated MIN6WT cells. In contrast, levels of eIF4G bound to eIF4E were not decreased by thapsigargin in MIN6*Eif4ebp1* $^{-/-}$ cells (Figure 3C, compare lane 7 with lane 8). Thus, eIF4E availability for translational initiation was greater in MIN6*Eif4ebp1* $^{-/-}$ cells than in MIN6*WT* cells under ER stress. Measurement of the global translation rate revealed that recovery from translational suppression by thapsigargin was more rapid in 4E-BP1-deficient cells (Figure 3D).

Translation of newly synthesized mRNA molecules is reportedly much more dependent on eIF4E availability than that of preexisting mRNAs (Novoa and Carrasco, 1999). Expression of CHOP, a mediator of ER stress-induced apoptosis, was thus studied in MIN6*Eif4ebp1* $^{-/-}$ cells since *Chop* mRNA is one of the transcripts most abundantly synthesized during ER stress (Pirot et al., 2007). *Eif4ebp1* deletion caused greater CHOP protein induction by thapsigargin in MIN6 cells (Figure 3E), with unaltered *Chop* mRNA accumulation (Figure 3F). Pulse-labeling experiments demonstrated enhanced CHOP translation (Figure 3G). Thus, CHOP expression during ER stress was augmented via increased translation in 4E-BP1 deficiency.

Eif4ebp1 Deletion Accelerates β Cell Loss in Mouse Diabetes Models

To examine the roles of 4E-BP1 under ER stress in vivo, *Eif4ebp1* $^{-/-}$ mice on the 129S6 background were fed a high-fat diet (HFD), which is thought to produce ER stress in β cells through peripheral insulin resistance (Scheuner et al., 2005). *Eif4ebp1* $^{-/-}$ mice developed glucose intolerance (Figures S4A and S4B), which was associated with blunted insulin secretion (Figure S4C) and reduced pancreatic insulin content (Figure S4D) as compared to HFD-fed wild-type mice. These data suggest that *Eif4ebp1* $^{-/-}$ mice have a β cell defect. However, HFD-fed *Eif4ebp1* $^{-/-}$ mice gained more weight and were more insulin resistant than HFD-fed wild-type mice (Figures S4E and S4F). Therefore, the possibility remains that β cell failure in HFD-fed *Eif4ebp1* $^{-/-}$ mice resulted from greater ER stress rather than from a defect in β cells lacking 4E-BP1.

We next crossed *Eif4ebp1* $^{-/-}$ mice with two genetic models of diabetes in which β cells are under ER stress, *Ins2* $^{WT/C96Y}$ and *Wfs1* $^{-/-}$ mice on the 129S6 background. 4E-BP1 deficiency did not alter body weight (Figures S5A and S5B) or insulin sensitivity (Figures S5C and S5D) but worsened hyperglycemia in *Ins2* $^{WT/C96Y}$ (Figure 4A) and *Wfs1* $^{-/-}$ (Figure 4B) mice. In *Eif4ebp1* $^{-/-}$ *Ins2* $^{WT/C96Y}$ mice, pancreatic insulin content was less than half of that in *Ins2* $^{WT/C96Y}$ mice at 5 weeks of age (Figure 4C), and the majority of islets in *Eif4ebp1* $^{-/-}$ *Ins2* $^{WT/C96Y}$ mice were smaller as compared to those in *Ins2* $^{WT/C96Y}$ mice (Figure 4D). We also observed a 38% decrease in pancreatic insulin content in *Eif4ebp1* $^{-/-}$ *Wfs1* $^{-/-}$ mice as compared to *Wfs1* $^{-/-}$ mice (Figure 4E). Importantly, the insulin-positive area was smaller in pancreatic sections from *Eif4ebp1* $^{-/-}$ *Wfs1* $^{-/-}$ mice than in pancreatic sections from *Wfs1* $^{-/-}$ mice at 27–30 weeks of age (Figure 4F), indicating that ER stress-mediated β cell loss is exacerbated by 4E-BP1 deficiency in vivo.

Global protein synthesis was studied in these mouse islets. A tendency toward decreased protein synthesis was observed in both *Ins2* $^{WT/C96Y}$ (Figure 4G, hatched bar; $p = 0.074$) and *Wfs1* $^{-/-}$ islets (Figure 4H, hatched bar; $p = 0.079$) as compared to wild-type islets. *Eif4ebp1* deletion ablated this regulation and resulted in significantly increased protein synthesis in *Eif4ebp1* $^{-/-}$ *Ins2* $^{WT/C96Y}$ ($p = 0.013$) and *Eif4ebp1* $^{-/-}$ *Wfs1* $^{-/-}$ ($p = 0.045$) islets as compared to that in corresponding single mutants (compared hatched with filled bars in Figures 4G and 4H). These data suggest that accelerated β cell loss under ER stress is due to deregulated translational control.

DISCUSSION

Our results implicate 4E-BP1, identified as a component of the UPR, in β cell survival under ER stress. Important roles of 4E-BPs under various stress conditions have been recently demonstrated in yeast (Ibrahimo et al., 2006) and *Drosophila* (Teleman et al., 2005; Tettweiler et al., 2005). These data suggest that translational suppression by 4E-BPs is an evolutionarily conserved strategy against stress conditions. Although we focused on β cells, ER stress-mediated induction of 4E-BP1 was also observed in the liver and kidneys, suggesting the general importance of the present findings.

Our results suggest that, in addition to translational regulation by eIF2α phosphorylation due to PERK activation, another mode of translational control mediated by 4E-BP1 plays a role in the maintenance of β cell homeostasis under ER stress. Since translational suppression by eIF2α phosphorylation is transient owing to feedback dephosphorylation by GADD34 (Novoa et al., 2001), prolonged translational suppression by 4E-BP1 might be needed in the later stages of the UPR. However, in contrast to PERK, 4E-BP1 deficiency alone does not cause diabetes in mice under normal conditions, suggesting that 4E-BP1 protein is not a key regulator but rather functions with other molecules to maintain β cell homeostasis under ER stress. The preferential role of 4E-BP1 in the later stages of the UPR might be puzzling since expression of

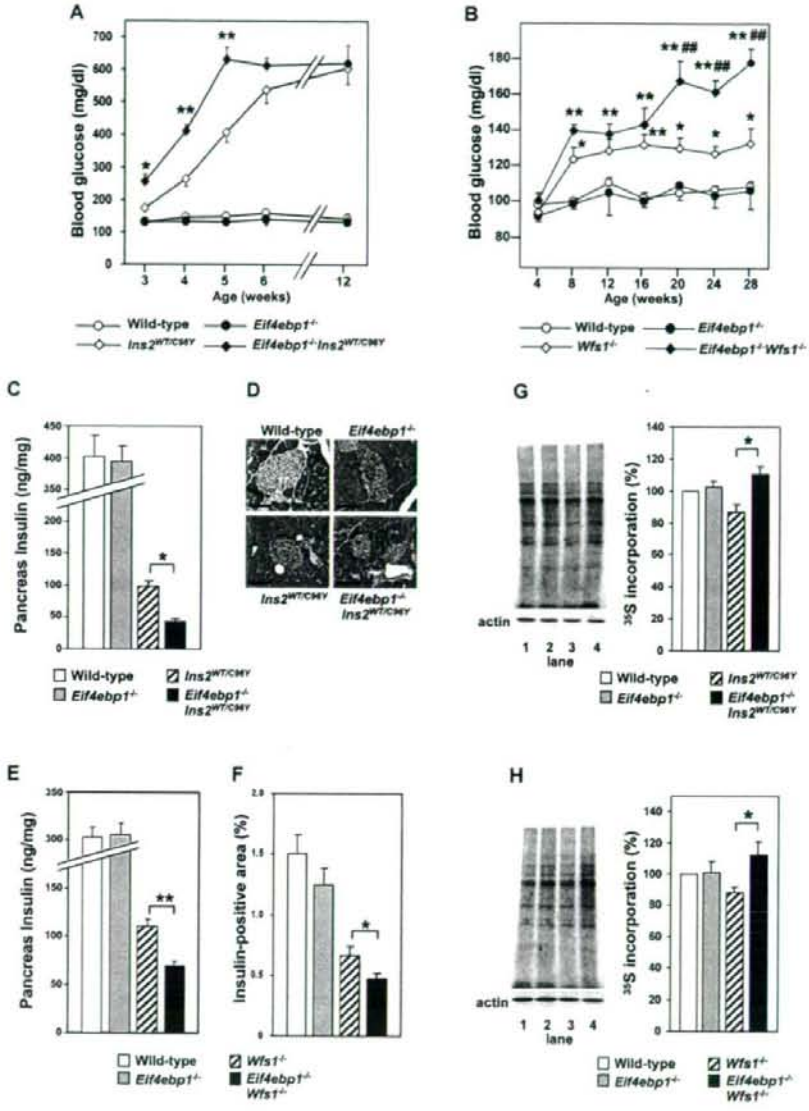

Figure 4. β Cell Loss Is Exacerbated by 4E-BP1 Deficiency in Mouse Diabetes Models

(A) Fed blood glucose levels of wild-type (n = 6), *Eif4ebp1*$^{-/-}$ (n = 5), *Ins2*$^{WT/C96Y}$ (n = 9), and *Eif4ebp1*$^{-/-}$ *Ins2*$^{WT/C96Y}$ (n = 11) mice. Data from three cohorts are combined. *p < 0.05, **p < 0.01 versus *Ins2*$^{WT/C96Y}$ mice.

(B) Fed blood glucose levels of wild-type (n = 12), *Eif4ebp1*$^{-/-}$ (n = 8), *Wfs1*$^{-/-}$ (n = 15), and *Eif4ebp1*$^{-/-}$ *Wfs1*$^{-/-}$ (n = 10) mice. Data from three cohorts are combined. *p < 0.05, **p < 0.01 versus wild-type mice; ##p < 0.01 versus *Wfs1*$^{-/-}$ mice.

(C) Pancreatic insulin content of mice of the indicated genotypes at 5 weeks of age. n = 3 for each genotype. *p < 0.05.

(D) Hematoxylin and eosin staining of sections showing representative islets from mice of the indicated genotypes at 5 weeks of age. Scale bars = 50 μm.

(E) Pancreatic insulin content of wild-type (n = 8), *Eif4ebp1*$^{-/-}$ (n = 4), *Wfs1*$^{-/-}$ (n = 15), and *Eif4ebp1*$^{-/-}$ *Wfs1*$^{-/-}$ (n = 12) mice at 27–30 weeks of age. **p < 0.01.

(F) Insulin-positive area in pancreatic sections of wild-type (n = 3), *Eif4ebp1*$^{-/-}$ (n = 3), *Wfs1*$^{-/-}$ (n = 4), and *Eif4ebp1*$^{-/-}$ *Wfs1*$^{-/-}$ (n = 5) mice at 27–30 weeks of age. *p < 0.05.

(G) [^{35}S]methionine/cysteine incorporation in islets of the indicated genotypes at 5–6 weeks of age. Ten percent of the lysates were also probed with an anti-actin antibody. A representative autoradiogram is shown in the left panel. Lane 1, wild-type; lane 2, *Eif4ebp1*$^{-/-}$; lane 3, *Ins2*$^{WT/C96Y}$; lane 4, *Eif4ebp1*$^{-/-}$ *Ins2*$^{WT/C96Y}$. Data from four experiments are summarized in the right panel. *p < 0.05.

ATF4, the primary inducer of *Eif4ebp1* under ER stress, is activated by translational suppression by eIF2α phosphorylation during the acute phase. We found that 4E-BP1 protein is stable with a half-life of approximately 20 hr (Figure S6). Thus, 4E-BP1 protein seems to continue to be expressed abundantly during the later stages of the UPR. This is consistent with the recent observation that several prosurvival proteins involved in the UPR are stable, while proapoptotic proteins are not (Rutkowski et al., 2006). We found that global protein synthesis was higher in 4E-BP1-deficient β cells than in wild-type cells under ER stress conditions. In particular, expression of CHOP was augmented in 4E-BP1 deficiency. Enhanced CHOP expression in 4E-BP1-deficient cells suggests that a reduction in eIF4E availability due to 4E-BP1 induction suppresses CHOP translation during ER stress in wild-type cells, possibly accounting for one of the mechanisms by which 4E-BP1 plays a role in adaptation to ER stress. Important roles of translational control via eIF4E availability have also been suggested in prolonged hypoxia (Koritzinsky et al., 2006). However, the signaling mechanisms for translational control are different: ER stress increases 4E-BP1 protein levels via ATF4 in β cells, while hypoxia enhances 4E-BP1 activity via dephosphorylation and also causes eIF4E nuclear localization in HeLa cells.

The present results also suggest that variations in genes regulating eIF4E availability and/or eIF4F formation may have an impact on susceptibility to diabetes. In this context, a recent report demonstrating that a gene encoding eIF4A2, a component of eIF4F, is possibly linked to type 2 diabetes in French families (Cheyssac et al., 2006) is of great interest. Furthermore, our findings raise the possibility that 4E-BP1 may be a potential target for diabetes mellitus treatment.

EXPERIMENTAL PROCEDURES

Animal Experiments

All animal experiments were approved by the Tohoku University Institutional Animal Care and Use Committee. *Wfs1*$^{-/-}$ mice were backcrossed to a 129S6 (Taconic) background for six generations. *Ins2*$^{WT/C96Y}$ mice (Charles River Laboratories) were backcrossed to a 129S6 background for five generations. *Eif4ebp1* $^{/}$ mice were maintained on a 129S6 background. Only male mice were used. For the in vivo studies shown in Figures 4A, 4C, and 4D, littermates from crosses of male *Ins2*$^{WT/C96Y}$ *Eif4ebp1*$^{+/-}$ and female *Ins2*$^{WT/WT}$ *Eif4ebp1*$^{+/-}$ mice were used. For Figures 4B, 4E, and 4F, littermates from intercrosses of *Eif4ebp1*$^{+/-}$ *Wfs1*$^{+/+}$ mice and littermates from intercrosses of *Eif4ebp1*$^{+/-}$ *Wfs1*$^{-/-}$ mice were used. For isolated islet experiments (Figures 4G and 4H), age-matched nonlittermate mice were used. To induce ER stress in vivo, mice were given a 0.5 μg/g body weight intraperitoneal injection of tunicamycin. After 96 hr, kidneys and livers were removed. Tissue sample processing, immunostaining of pancreatic sections, and determination of β cell area and pancreatic insulin content were performed as described previously (Ishihara et al., 2004).

Cell Culture and Cell Viability Assay

Pancreatic tumors in *Eif4ebp1*$^{-/-}$;SV40Tag mice on a mixed background were excised, yielding MIN6*Eif4ebp1* $^{/}$ cells, which were used at 5–10 passages in this study. MIN6 cells were cultured in DMEM supplemented with 15% FCS. *Atf4*$^{-/-}$ MEFs were cultured in DMEM supplemented with a nonessential amino acid mixture and 10% FCS. Cells seeded in 24-well plates 2 days previously were treated with thapsigargin or tunicamycin and used for western blotting or cell viability assay. Cell viability was determined with a cell proliferation assay kit (Promega). Construction of adenoviruses and infection of MIN6 cells were performed as described previously (Ishihara et al., 2004).

Northern and Western Blotting and Cap-Binding Affinity Assay

Total RNA extracted using ISOGEN (Nippon Gene) was probed with ^{32}P-labeled cDNAs. Tissue homogenates and cell lysates were subjected to SDS-PAGE and probed with primary antibodies against 4E-BP1, 4E-BP2, eIF4E, eIF4G, cleaved caspase-3 (Cell Signaling), ATF4, CHOP (Santa Cruz), and actin (Sigma). Cell lysates were incubated with 7-methyl-GTP (^{7}mGTP)-Sepharose (Amersham) overnight at 4°C. The ^{7}mGTP-Sepharose was then pelleted and boiled. Experiments were performed at least three times. Band intensity was quantified using Scion Image software.

Metabolic Labeling

Due to the low islet yields from *Ins2*$^{WT/C96Y}$, *Ins2*$^{WT/C96Y}$ *Eif4ebp1* $^{/}$, *Wfs1* $^{/}$, and *Eif4ebp1* $^{/}$ *Wfs1* $^{/}$ mice, islets with these genotypes were pooled from two or three mice. Fifty to eighty islets were cultured for 3 days in RPMI supplemented with 10% FCS. Islets washed with methionine/cysteine-free RPMI containing 10% dialyzed FCS were labeled with a protein labeling mix (PerkinElmer) (1.0 MBq/tube) for 15 min and then resolved in sample buffer (1.0 μl/islet for wild-type and *Eif4ebp1* $^{/}$ islets and 0.75 μl/islet for other genotypes). The level of protein synthesis was quantified from autoradiograms. For measurement of *Chop* translation, 4 × 10^{6} cells treated with thapsigargin for 12 hr were washed with methionine/cysteine-free DMEM containing 15% dialyzed FCS and labeled with [^{35}S]methionine/cysteine (20 MBq/bottle) for 2 hr. Cells were then resolved in lysis buffer (50 mM Tris [pH 7.5], 150 mM NaCl, 2 mM $MgCl_2$, 0.1% Triton X-100, and protease inhibitors [Roche]). Lysates were precleared with Protein A Sepharose Fast Flow (Amersham) and incubated with anti-CHOP antibody (R-20, Santa Cruz) overnight.

Firefly Luciferase Reporter Assay

Oligonucleotides containing ATF4 binding sites were annealed and subcloned into the pGL3-Promoter vector (BamHI-SalI, Promega). MIN6 cells were transfected with luciferase reporters using Lipofectamine (Invitrogen). Luciferase activity was assayed with a dual-luciferase system (Promega) using a luminometer (Berthold).

Chromatin Immunoprecipitation Assay

Proteins bound to DNA were crosslinked with 1% formaldehyde at 4°C for 20 min. After sonication, the protein-DNA complexes were immunoprecipitated using an anti-ATF4 antibody (C-20, Santa Cruz). After reversal of the crosslinks at 65°C for 6 hr, DNA was purified on a DNA purification column (QIAGEN). PCR was performed with the primers 5′-GATGAGGAAGAGGAAGCTGAGT TG-3′ and 5′-AGTTGTAAGAGGAGTAGTTGGGGG-3′.

Statistical Analysis

Data are presented as means ± SEM. Differences between groups were assessed by Student's t test. $p < 0.05$ was considered significant.

SUPPLEMENTAL DATA

Supplemental Data include six figures and Supplemental References and can be found with this article online at http://www.cellmetabolism.org/cgi/content/full/7/3/269/DC1/.

ACKNOWLEDGMENTS

We thank J. Alam (Alton Ochsner Medical Foundation) and D. Ron (New York University) for their generous gifts of DN-ATF4 cDNA and *Atf4*$^{-/-}$ MEFs, respectively. We are also grateful to K. Igarashi (Tohoku University) for advice on ChIP analysis and to Y. Nagura and K. Tanaka for their expert technical assistance. This work was supported by Grants-in-Aid for Scientific Research

(H) [^{35}S]methionine/cysteine labeling as in (G) in islets of the indicated genotypes at 6–8 weeks of age. Lane 1, wild-type; lane 2, *Eif4ebp1*$^{-/-}$; lane 3, *Wfs1*$^{-/-}$; lane 4, *Eif4ebp1*$^{-/-}$ *Wfs1*$^{-/-}$. Data from three experiments are summarized in the right panel. *$p < 0.05$.
Error bars represent SEM.

(19590300 to H.I. and 19209034 to Y.O.) from the Ministry of Education, Culture, Sports, Science and Technology of Japan.

Received: July 10, 2007
Revised: December 2, 2007
Accepted: January 30, 2008
Published: March 4, 2008

REFERENCES

Butler, A.E., Janson, J., Bonner-Weir, S., Ritzel, R., Rizza, R.A., and Butler, P.C. (2003). β-cell deficit and increased beta-cell apoptosis in humans with type 2 diabetes. Diabetes *52*, 102–110.

Cheyssac, C., Dina, C., Lepretre, F., Vasseur-Delannoy, V., Dechaume, A., Lobbens, S., Balkau, B., Ruiz, J., Charpentier, G., Pattou, F., et al. (2006). EIF4A2 is a positional candidate gene at the 3q27 locus linked to type 2 diabetes in French families. Diabetes *55*, 1171–1176.

Clemens, M.J. (2001). Translational regulation in cell stress and apoptosis. Roles of the eIF4E binding proteins. J. Cell. Mol. Med. *5*, 221–239.

Delepine, M., Nicolino, M., Barrett, T., Golamaully, M., Lathrop, G.M., and Julier, C. (2000). EIF2AK3, encoding translation initiation factor 2-alpha kinase 3, is mutated in patients with Wolcott-Rallison syndrome. Nat. Genet. *25*, 406–409.

Harding, H.P., Novoa, I., Zhang, Y., Zeng, H., Wek, R., Schapira, M., and Ron, D. (2000). Regulated translation initiation controls stress-induced gene expression in mammalian cells. Mol. Cell *6*, 1099–1108.

Harding, H.P., Zeng, H., Zhang, Y., Jungries, R., Chung, P., Plesken, H., Sabatini, D.D., and Ron, D. (2001). Diabetes mellitus and exocrine pancreatic dysfunction in perk−/− mice reveals a role for translational control in secretory cell survival. Mol. Cell *7*, 1153–1163.

Harding, H.P., Zhang, Y., Zeng, H., Novoa, I., Lu, P.D., Calfon, M., Sadri, N., Yun, C., Popko, B., Paules, R., et al. (2003). An integrated stress response regulates amino acid metabolism and resistance to oxidative stress. Mol. Cell *11*, 619–633.

He, C.H., Gong, P., Hu, B., Stewart, D., Choi, M.E., Choi, A.M., and Alam, J. (2001). Identification of activating transcription factor 4 (ATF4) as an Nrf2-interacting protein. Implication for heme oxygenase-1 gene regulation. J. Biol. Chem. *276*, 20858–20865.

Holcik, M., and Sonenberg, N. (2005). Translational control in stress and apoptosis. Nat. Rev. Mol. Cell Biol. *6*, 318–327.

Ibrahimo, S., Holmes, L.E., and Ashe, M.P. (2006). Regulation of translation initiation by the yeast eIF4E binding proteins is required for the pseudohyphal response. Yeast *23*, 1075–1088.

Inoue, H., Tanizawa, Y., Wasson, J., Behn, P., Kalidas, K., Bernal-Mizrachi, E., Mueckler, M., Marshall, H., Donis-Keller, H., Crock, P., et al. (1998). A gene encoding a transmembrane protein is mutated in patients with diabetes mellitus and optic atrophy (Wolfram syndrome). Nat. Genet. *20*, 143–148.

Ishihara, H., Takeda, S., Tamura, A., Takahashi, R., Yamaguchi, S., Takei, D., Yamada, T., Inoue, H., Soga, H., Katagiri, H., et al. (2004). Disruption of the WFS1 gene in mice causes progressive beta-cell loss and impaired stimulus-secretion coupling in insulin secretion. Hum. Mol. Genet. *13*, 1159–1170.

Koritzinsky, M., Magagnin, M.G., van den Beucken, T., Seigneuric, R., Savelkouls, K., Dostie, J., Pyronnet, S., Kaufman, R.J., Weppler, S.A., Voncken, J.W., et al. (2006). Gene expression during acute and prolonged hypoxia is regulated by distinct mechanisms of translational control. EMBO J. *25*, 1114–1125.

Laybutt, D.R., Preston, A.M., Akerfeldt, M.C., Kench, J.G., Busch, A.K., Biankin, A.V., and Biden, T.J. (2007). Endoplasmic reticulum stress contributes to beta cell apoptosis in type 2 diabetes. Diabetologia *50*, 752–763.

Miyazaki, J., Araki, K., Yamato, E., Ikegami, H., Asano, T., Shibasaki, Y., Oka, Y., and Yamamura, K. (1990). Establishment of a pancreatic beta cell line that retains glucose-inducible insulin secretion: special reference to expression of glucose transporter isoforms. Endocrinology *127*, 126–132.

Novoa, I., and Carrasco, L. (1999). Cleavage of eukaryotic translation initiation factor 4G by exogenously added hybrid proteins containing poliovirus 2Apro in HeLa cells: effects on gene expression. Mol. Cell. Biol. *19*, 2445–2454.

Novoa, I., Zeng, H., Harding, H.P., and Ron, D. (2001). Feedback inhibition of the unfolded protein response by GADD34-mediated dephosphorylation of eIF2α. J. Cell Biol. *153*, 1011–1022.

Pirot, P., Naamane, N., Libert, F., Magnusson, N.E., Orntoft, T.F., Cardozo, A.K., and Eizirik, D.L. (2007). Global profiling of genes modified by endoplasmic reticulum stress in pancreatic beta cells reveals the early degradation of insulin mRNAs. Diabetologia *50*, 1006–1014.

Riggs, A.C., Bernal-Mizrachi, E., Ohsugi, M., Wasson, J., Fatrai, S., Welling, C., Murray, J., Schmidt, R.E., Herrera, P.L., and Permutt, M.A. (2005). Mice conditionally lacking the Wolfram gene in pancreatic islet beta cells exhibit diabetes as a result of enhanced endoplasmic reticulum stress and apoptosis. Diabetologia *48*, 2313–2321.

Rutkowski, D.T., Arnold, S.M., Miller, C.N., Wu, J., Li, J., Gunnison, K.M., Mori, K., Sadighi Akha, A.A., Raden, D., and Kaufman, R.J. (2006). Adaptation to ER stress is mediated by differential stabilities of pro-survival and pro-apoptotic mRNAs and proteins. PLoS Biol. *4*, e374.

Scheuner, D., Mierde, D.V., Song, B., Flamez, D., Creemers, J.W., Tsukamoto, K., Ribick, M., Schuit, F.C., and Kaufman, R.J. (2005). Control of mRNA translation preserves endoplasmic reticulum function in β cells and maintains glucose homeostasis. Nat. Med. *11*, 757–764.

Schroder, M., and Kaufman, R.J. (2005). The mammalian unfolded protein response. Annu. Rev. Biochem. *74*, 739–789.

Strom, T.M., Hortnagel, K., Hofmann, S., Gekeler, F., Scharfe, C., Rabl, W., Gerbitz, K.D., and Meitinger, T. (1998). Diabetes insipidus, diabetes mellitus, optic atrophy and deafness (DIDMOAD) caused by mutations in a novel gene (wolframin) coding for a predicted transmembrane protein. Hum. Mol. Genet. *7*, 2021–2028.

Teleman, A.A., Chen, Y.W., and Cohen, S.M. (2005). 4E-BP functions as a metabolic brake used under stress conditions but not during normal growth. Genes Dev. *19*, 1844–1848.

Tettweiler, G., Miron, M., Jenkins, M., Sonenberg, N., and Lasko, P.F. (2005). Starvation and oxidative stress resistance in Drosophila are mediated through the eIF4E-binding protein, d4E-BP. Genes Dev. *19*, 1840–1843.

Tsukiyama-Kohara, K., Poulin, F., Kohara, M., DeMaria, C.T., Cheng, A., Wu, Z., Gingras, A.C., Katsume, A., Elchebly, M., Spiegelman, B.M., et al. (2001). Adipose tissue reduction in mice lacking the translational inhibitor 4E-BP1. Nat. Med. *7*, 1128–1132.

Wang, J., Takeuchi, T., Tanaka, S., Kubo, S.K., Kayo, T., Lu, D., Takata, K., Koizumi, A., and Izumi, T. (1999). A mutation in the insulin 2 gene induces diabetes with severe pancreatic β-cell dysfunction in the Mody mouse. J. Clin. Invest. *103*, 27–37.

Zhang, P., McGrath, B., Li, S., Frank, A., Zambito, F., Reinert, J., Gannon, M., Ma, K., McNaughton, K., and Cavener, D.R. (2002). The PERK eukaryotic initiation factor 2α kinase is required for the development of the skeletal system, postnatal growth, and the function and viability of the pancreas. Mol. Cell. Biol. *22*, 3864–3874.

Available online at www.sciencedirect.com
ScienceDirect
Neuroscience Research 61 (2008) 143–158
Neuroscience Research
www.elsevier.com/locate/neures

Behavioral and gene expression analyses of *Wfs1* knockout mice as a possible animal model of mood disorder

Tadafumi Kato [a,*], Mizuho Ishiwata [a], Kazuyuki Yamada [b], Takaoki Kasahara [a], Chihiro Kakiuchi [a], Kazuya Iwamoto [a], Koki Kawamura [c], Hisamitsu Ishihara [d], Yoshitomo Oka [d]

[a] *Laboratory for Molecular Dynamics of Mental Disorders, RIKEN Brain Science Institute, Hirosawa 2-1, Wako, Saitama 351-0198, Japan*
[b] *Support Unit for Animal Experiment, RIKEN Brain Science Institute, Wako, Saitama 351-0198, Japan*
[c] *Laboratory for Cell Culture Development, RIKEN Brain Science Institute, Wako, Saitama 351-0198, Japan*
[d] *Division of Molecular Metabolism and Diabetes, Tohoku University Graduate School of Medicine, Sendai, Japan*

Received 21 November 2007; accepted 7 February 2008
Available online 14 February 2008

Abstract

Wolfram disease is a rare genetic disorder frequently accompanying depression and psychosis. Non-symptomatic mutation carriers also have higher rates of depression and suicide. Because *WfS1*, the causative gene of Wolfram disease, is located at 4p16, a linkage locus for bipolar disorder, mutations of *WfS1* were suggested to be involved in the pathophysiology of bipolar disorder. In this study, we performed behavioral and gene expression analyses of *Wfs1* knockout mice to assess the validity as an animal model of mood disorder. In addition, the distribution of *Wfs1* protein was examined in mouse brain. *Wfs1* knockout mice did not show abnormalities in circadian rhythm and periodic fluctuation of wheel-running activity. Behavioral analysis showed that *Wfs1* knockout mice had retardation in emotionally triggered behavior, decreased social interaction, and altered behavioral despair depending on experimental conditions. *Wfs1*-like immunoreactivity in mouse brain showed a similar distribution pattern to that in rats, including several nuclei potentially relevant to the symptoms of mood disorders. Gene expression analysis showed down-regulation of *Cdc42ep5* and *Rnd1*, both of which are related to Rho GTPase, which plays a role in dendrite development. These findings may be relevant to the mood disorder observed in patients with Wolfram disease.

Keywords: Wolframin; Wolfram disease; Depression; Bipolar disorder; DNA microarray; Forced swimming test

1. Introduction

Wolfram disease (Online Mendelian Inheritance in Man [OMIM] 222300) is a rare autosomal recessive neurodegenerative disorder characterized by early-onset diabetes mellitus, progressive optic atrophy, diabetes insipidus, and deafness (Domenech et al., 2006); *WfS1/wolframin* has been identified as the causative gene (Strom et al., 1998; Inoue et al., 1998). Approximately, 60% of the patients with Wolfram disease have mental symptoms, such as severe depression, psychosis, impulsivity, and aggression (Swift et al., 1990). More importantly, carriers of *WfS1* mutations, who are not affected with Wolfram disease, have a 26-fold higher likelihood of psychiatric hospitalization mainly due to depression (Swift and Swift, 2000). The *WfS1* gene locates at 4p16.1 (Strom et al., 1998; Inoue et al., 1998), a replicated linkage locus of bipolar disorder (Ewald et al., 1998, 2002; Detera-Wadleigh et al., 1999). Some studies showed that bipolar disorder with psychosis (Als et al., 2004; Cheng et al., 2006) or suicidal behavior (Cheng et al., 2006) is linked with this locus. These lines of evidence suggested the possible role of *WfS1* mutations in the pathophysiology of bipolar disorder and related phenotypes.

To date, mutation screening of the *WfS1* gene has been reported in 84 patients with bipolar disorder, 54 with major depression, 119 with schizophrenia, 100 suicide victims, 3 with schizoaffective disorder, and several other patients with other psychiatric diagnoses (Ohtsuki et al., 2000; Martorell et al., 2003; Torres et al., 2001; Crawford et al., 2002; Evans et al., 2000). However, none of these patients had mutations causing Worfram disease.

* Corresponding author. Tel.: +81 48 467 6949; fax: +81 48 467 6947.
E-mail address: kato@brain.riken.jp (T. Kato).

0168-0102/$ – see front matter © 2008 Published by Elsevier Ireland Ltd and the Japan Neuroscience Society.
doi:10.1016/j.neures.2008.02.002

Despite the fact that *WfS1* mutations may not be a frequent cause of mental disorders, the mechanism underlying how *WfS1* mutations lead to mental symptoms in patients with Wolfram disease will shed light on the pathophysiology of mood disorders. Mice lacking the *Wfs1* gene might be useful as a genetic animal model of mood disorders.

The symptoms of Wolfram disease resemble those of mitochondrial diseases and, indeed, initial studies suggested mitochondrial dysfunction in Wolfram disease based on mitochondrial DNA (mtDNA) deletions found in patients (Rotig et al., 1993). However, the protein coded by *WfS1* was found to be localized in endoplasmic reticulum (ER) (Takeda et al., 2001; Philbrook et al., 2005). *WfS1* expression was induced by ER stress (Fonseca et al., 2005) or *XBP1* overexpression (Kakiuchi et al., 2006), and disruption of *Wfs1* caused a dysfunctional ER stress response (Fonseca et al., 2005; Riggs et al., 2005; Yamada et al., 2006). Recent studies have provided insight into the function of *WfS1* protein; *WfS1* induces cation channel activity on ER membranes (Osman et al., 2003) and regulates calcium levels in ER (Takei et al., 2006). It also plays a role in stimulus-secretion coupling for insulin exocytosis in pancreatic β cells (Ishihara et al., 2004). Disruption of *Wfs1* increased vulnerability to cell death in the knockout (KO) mice (Ishihara et al., 2004; Philbrook et al., 2005; Riggs et al., 2005; Yamada et al., 2006). In the rat brain, *WfS1* was distributed predominantly in neurons of the so-called limbic system (Takeda et al., 2001). *WfS1* mutations could lead to loss of *WfS1*-expressing neurons in particular brain regions of patients with Wolfram disease, which may underlie progression of mental symptoms.

In this study, we performed behavioral analysis of *Wfs1* KO mice to characterize their behavioral abnormality. We previously developed neuron-specific mutant polymerase γ-transgenic mice (mPolg Tg mice) based on a mitochondrial dysfunction hypothesis of bipolar disorder (Kato and Kato, 2000) and demonstrated that these mice had bipolar disorder-like phenotypes, such as altered circadian rhythm and periodic fluctuation of wheel-running activity (Kasahara et al., 2006). Whether or not the *Wfs1* KO mice show such wheel-running activity was examined. A behavioral test battery was also conducted to search for other behavioral phenotypes. Distribution of *Wfs1* in the brain was examined to search for the neural basis of behavioral alteration. In addition, gene expression analysis was performed to search for the molecular basis of behavioral phenotypes of *Wfs1* KO mice.

2. Experimental procedures

2.1. Generation of Wfs1 KO mice

The methods for the generation of *Wfs1* KO mice have been described elsewhere (Ishihara et al., 2004). In brief, a neomycin-resistance gene was inserted into exon 2 of the *Wfs1* gene in the targeting vector. The targeting vector was injected into 129Sv embryonic stem (ES) cells, and the ES cells with homologous recombination were obtained. By crossing the chimeric mice with C57BL/6J (B6) mice, *Wfs1* heterozygous KO mice were obtained. Genotyping was performed as previously described (Ishihara et al., 2004). The heterozygous KO mice were crossed with the B6 mice for at least eight generations before the analysis. The mice were maintained in a 12-h light:12-h dark cycle, except for several specific experiments as indicated. Wild-type (WT) littermates were used for the control whenever possible. All animal experiments were approved by the local animal experiment committees of RIKEN and Behavioral and Medical Sciences Research Consortium (BMSRC) (Akashi, Japan). Animal experiments were carried out in accordance with the National Institute of Health Guide for the Care and Use of Laboratory Animals. All efforts were made to minimize the number of animals used and their suffering.

2.2. Wheel-running activity

For this analysis, 11 homozygous KO mice ($Wfs1^{-/-}$) and 9 WT littermates ($Wfs1^{+/+}$) were used. All were males aged 34 weeks at the initiation of the analysis. The groups did not differ significantly in body weight.

The methods for the analysis of wheel-running activity were described in detail elsewhere (Kasahara et al., 2006). In brief, mice were individually housed in cages (width, 24 cm; depth, 11 cm; height, 14 cm) equipped with a steel wheel (width, 5 cm; diameter, 14 cm) (O'Hara & Co., Tokyo, Japan). Wheel-running activity was monitored by measuring the rotation of the wheel (3 counts/1 rotation). Food and water were available ad libitum. The data of initial 7–10 days were omitted from the analysis. Delayed and anticipatory activity indices, referring to the wheel-running activity during the initial 3 h of a light phase and that during the last 3 h of a light phase, were calculated. The periodicity of wheel-running activity was assessed by Lomb-Scargle periodogram (Kasahara et al., 2006).

The Mann–Whitney *U*-test was used for statistical analyses. Significance levels were set at 0.05 (two-tailed; d.f., degree of freedom). The average and standard error of mean (S.E.M.) were presented for each experimental parameter in one group.

2.3. Behavioral analysis: phase I. Screening by a test battery

This analysis was performed at BMSRC (Akashi, Japan). For this analysis, 14 homozygous KO mice ($Wfs1^{-/-}$), 14 heterozygous KO mice ($Wfs1^{-/+}$), and 13 WT littermates ($Wfs1^{+/+}$) were analyzed. All were males aged 12 weeks at the initiation of the behavioral analysis. The analyses were performed in the order of open-field test, startle response and prepulse inhibition test, elevated plus maze, Morris water maze, passive avoidance learning, active avoidance learning, and forced swimming test. After the behavioral test battery, the non-fasting blood glucose level was examined to rule out the possibility that elevated blood glucose levels might affect the results of behavioral analysis. There was no significant difference among the genotypes, consistent with a previous report that there was no apparent increase in blood glucose levels in *Wfs1* KO mice on the B6 background (Ishihara et al., 2004).

2.3.1. Open-field test

A transparent cubic box without a ceiling (30 cm × 30 cm × 30 cm) was placed in a ventilated sound-attenuating chamber. A 40-W white lamp provided room lighting, which was approximately 110 lx on the floor of the chamber. In addition, a fan attached on the upper part of the wall at one end of the chamber presented a masking noise of 45 dB. Two infrared beams were set on each wall 2 cm above the floor with an interval of 10 cm. The total number of successive interceptions of two adjoining beams on each bank was scored as locomotion behavior. The other 12 infrared ray beams were attached 4.5 cm above the floor in 2.5-cm intervals, and the total number of vertical beam interceptions was scored as rearing behavior. Each mouse was allowed to explore freely in the open-field area for 20 min.

For statistical analysis, repeated measures analysis of variance (ANOVA) with the intrasubject factor of time (1–20 min) and the intersubject factor of genotype (−/−, +/−, and +/+) was applied.

2.3.2. Startle response and prepulse inhibition (PPI)

Each mouse was enclosed in a transparent acrylic box (7 cm × 7 cm × 10 cm). Startle response was detected as vibration of the box, using an accelerometer (GH-313A, Keyence, Osaka, Japan). The acoustic startle pulse of broadband burst (115 dB, 50 ms) and tone prepulse (85 dB, 30 ms) were presented via a speaker located in front of the box. Light prepulse (30 ms) was

applied by LED. At the beginning of the session, 40 startle pulses were presented to test for basal startle responsiveness and its habituation. The average values of eight blocks, consisting of five startle pulses each, were used for the statistical analysis. After that, three different types of trials were performed: startle pulse alone ($n = 12$), startle pulse preceded by a tone prepulse ($n = 12$), and startle pulse preceded by a light prepulse ($n = 12$). Prepulses were presented 50, 100, or 200 ms before the startle pulse. In total, six types of prepulse ($n = 4$, each) were applied. The mean interval averaged 25 s (15–45 s) throughout the session. The startle response was recorded for 200 ms with the sampling frequency of 1000 Hz. The PPI was assessed by the ratio of the mean response of trials with one type of prepulse ($n = 4$) divided by the mean response of trials without prepulse ($n = 12$). Because light prepulse did not attenuate the startle response at all, only the data of tone prepulse were presented.

2.3.3. Elevated plus maze

The maze consisted of four arms, two open arms and two closed arms, 5 cm wide and 30 cm long with a gray acrylic floor, that met at a 10 cm × 10 cm center zone. Two closed arms had the transparent walls of 15 cm height on both sides, and the open arms had the low walls of 3 mm height on the both sides. The apparatus was mounted 75 cm above the floor of the room. The room lighting was approximately 20 lx on the maze. The video camera was placed 80 cm above the maze. A fan generated a masking noise of 45 dB. The animal was placed gently onto the center of the maze and was allowed to explore the maze freely for 10 min. Number of entries into each arm and time spent in each arm were recorded from videotapes.

2.3.4. Morris water maze

A round pool, with the diameter of 95 cm and the depth of 21.5 cm, was placed in the center of a 140 cm × 130 cm room. A platform with the diameter of 11 cm was set in one of quadrants and 5 mm beneath the surface of black water maintained at 21 ± 1 °C. On the first to fifth days, five trials per day were performed for learning phase. The mouse was released on one of three quadrants of the pool without the platform, and the time to reach the platform was measured. When the mouse could not reach the platform within 60 s, the experimenter placed the mouse on the platform. On the sixth day, a probe test was performed to examine whether the mouse remembered the place of the platform. The mouse was released in the quadrant on the opposite side of the platform and its behavior for 60 s was videotaped. The time staying in the target quadrant, where the platform had been placed, and immobility time were measured.

2.3.5. Passive avoidance learning

A mouse was placed in a box, consisting of two rooms separated by a shutter, that is, light and dark compartments (10 cm × 10 cm each). In the acquisition trial, the mouse was kept in the light compartment. Five seconds later, the door to the dark compartment was opened. When the mouse moved into the dark compartment, the shutter was closed, and 10 s later, an electrical shock (160 V, 3 s) was delivered through the grid floor. Twenty-four hours later, each mouse was placed again in the light compartment and the latency to enter the dark compartment was recorded up to a maximum of 180 s.

2.3.6. Active avoidance learning

The same apparatus with the one used for passive avoidance learning was used, but there was no shutter between the light and dark compartments. The box was set in a soundproof chamber, and illuminated by a 20 W white light set on the chamber. The ceiling of the dark room is made of a black acryl board, and the ceiling of the light room was a transparent acryl board.

The training was performed for 3 days. On each day, one session consisting of 50 trials was performed. In each trial, a condition stimulus (CS) of 1500 Hz sound (85 dB) was followed by an unconditioned stimulus (US) of 140-V electrical shock. The US was given 5 s after the initiation of the CS and continued until the mouse escaped to the other compartment. If the mouse did not move to the other compartment, the US lasted 15 s together with the CS. If the mouse moved within 5 s after the CS, CS was stopped and no US was given. None of the mice experienced the maximum length of the CS. The time from the CS to the escape and the number of escapes were used for the performance of learning.

2.3.7. Forced swimming test

Animals were thrown into a square pool 24 cm × 24 cm in size. The water was maintained constant at 21 °C. On the first day, the mice were left in the pool for 20 min, and the mobility during the first 5 min recorded by videocamera was assessed. On the second day, animals were thrown into the pool for 5 min and the immobility time during the 5 min was recorded. The immobility was defined by the two criteria. (1) No movement of all legs and the tail. (2) Completely stationary state in the pool, or the movement only by inertia by the adjacent movement. The immobility was assessed by three independent raters by scrutinizing the video and the median value of the three raters was used for the analysis.

2.4. Behavioral analysis: phase II

This analysis was performed at the Support Unit for Animal Experiment, RIKEN BSI. For this analysis, 9 homozygous KO mice (*Wfs1*$^{-/-}$) and 11 WT littermates (*Wfs1*$^{+/+}$) were analyzed. All were males aged 31 weeks at the initiation of the behavioral analysis. There was no significant difference of body weight at the initiation of the behavioral tests.

The analyses were performed in the order of home cage activity, open-field test, light-dark (L-D) box test, elevated plus maze, startle response and PPI test, Morris water maze, and fear conditioning. After each trial (except the auditory startle response and the water maze), apparatuses were wiped and cleaned by 80% alcohol and damp towel. For data acquisition, the Image J program (http://rsb.info.Nih.gov/ij) was used after some modification.

2.4.1. Environment of behavioral laboratory and housing condition of mice

Mice were housed individually for several days before they were transferred to the behavioral laboratory. The laboratory was air-conditioned and maintained temperature and humidity within approximately 22–23 °C and 50–55%. Food and water were freely available except during experimentation. Large tweezers were used to handle mice to avoid individual differences in the handling procedure. All of the experiments were conducted in the light phase (9:00–18:00 h), and the starting times of the experiments were kept constant.

2.4.2. Home cage activity measurement

Spontaneous activity of mice in their home cage was measured using a 24-ch ABsystem 4.0 (Neuroscience, Tokyo, Japan). Cages were individually set into the compartments made of stainless steel in the negative pressure rack (BCI., Tokyo, Japan). An infrared sensor was equipped on the ceiling of each compartment and it detected movements of the mice. Home cage activity was measured for 1 week from the afternoon of the day of transferring to the behavioral laboratory (day 1) until the next day of the week (day 8). After the termination of home cage activity measurement, cages and bedding materials were changed to fresh ones and then mice were maintained in the micro-isolation rack (Allentown Inc., Allentown, PA, USA), the same as those used in breeding rooms throughout the behavioral screening.

2.4.3. Open-field test

Four days after the termination of home cage activity measurement (day 12), an open-field test was conducted. The detailed protocol is shown in the supplementary information.

2.4.4. L-D box test

The next day (day 13) after the open-field test, an L-D box test was conducted. A four-channel of the L-D box system was equipped in the same sound-proof room as the open field. Each light box was made of white plastic (20 cm × 20 cm × 20 cm [H]) and illuminated by LEDs (250 lx at the center of the box); a CCD camera was equipped on the ceiling. Each dark box was made of black plastic (20 cm × 20 cm × 20 cm [H]) and an infrared camera was equipped on the ceiling. There was a tunnel for transition on the center panel between the light box and dark box (3 cm × 5 cm) with an automatic sliding door. In the L-D box test, mice were individually introduced into the light box, and the door of the tunnel automatically opened 3 s after the introduction of a mouse. Then mouse was allowed to move freely in the L-D box for 10 min. Total distance traveled, percent distance traveled in the light

box, percent duration staying in the light box, numbers of the transition between light and dark box, and the first latency to enter the dark box were measured as indices.

2.4.5. Elevated plus maze test

The next day (day 14) after the L-D box test, an elevated plus maze test was conducted. The detailed protocol is shown in the supplementary information.

2.4.6. Auditory startle response

The next day after the L-D box test, an auditory startle response test was conducted for 2 days. The detailed protocol is shown in the supplementary information.

2.4.7. The Morris water maze test

Three days after the termination of the auditory startle response test (day 18), a series of the Morris water maze test began. The detailed protocol is shown in the supplementary information.

2.4.8. Classical fear conditioning

Three days after the termination of the Morris water maze test (day 25), a classical fear-conditioning test was conducted. This test consisted of three parts: a conditioning trial (day 25), a context test trial (day 26), and a cued test trial (day 27). Fear conditioning was carried out on a clear plastic chamber equipped with a stainless steel grid floor (34 cm × 26 cm × 30 cm [H]). A CCD camera was equipped on the ceiling of the chamber and was connected to a video monitor and computer. The grid floor was wired to a shock generator. White noise (65 dB) was supplied from a loudspeaker as an auditory cue (CS). The conditioning trial consisted of a 2-min exploration period followed by two CS-US pairings separated by 1 min each. A US (foot-shock: 0.5 mA, 2 s) was administered at the end of the 30-s CS period. A context test was performed in the same conditioning chamber for 3 min in the absence of the white noise at 24 h after the conditioning trial. Further, a cued test was performed in an alternative context with distinct cues; the test chamber was different from the conditioning chamber in brightness (almost 0–1 lx), color (white), floor structure (no grid), and shape (triangular). The cued test was conducted 24 h after the contextual test was finished and consisted of a 2-min exploration period (no CS) to evaluate the non-specific contextual fear followed by a 2-min CS period (no foot shock) to evaluate the acquired cued fear. Rate of freezing response of mice was measured as an index of fear memory.

2.5. Behavioral analysis: phase III

This analysis was performed at the Support Unit for Animal Experiment, RIKEN BSI. For this analysis, seven homozygous KO mice (*Wfs1*$^{-/-}$) and eight WT littermates (*Wfs1*$^{+/+}$) were analyzed. All were males aged 9 weeks at the initiation of the behavioral analysis. There was no significant difference of body weight at the initiation of the behavioral tests (WT, 25.2 ± 0.6 g; KO, 25.2 ± 0.5 g).

The analyses were performed in the order of social interaction, rotarod test, sucrose preference test, tail suspension test, forced swimming test, marble burying test, hot plate test, and tail flick test. Inter-test intervals were 1 day to a week. After each trial (except the auditory startle response and the water maze), apparatuses were wiped and cleaned by 80% alcohol and damp towel. For data acquisition, the Image J program was used after some modification.

2.5.1. Social interaction test (encounter method)

Subject mice were individually put into the center of a white-colored open field (40 cm × 40 cm × 30 cm [H]). Immediately after the introduction of the subject mouse, a target mouse was also introduced into the same open field. The duration of contact behavior was measured for 60 min to assess passive contact. Contact or separation of mice was expressed as "1" or "2" by computerized image analysis. If the two mice contacted, the software return value of "1," and if separated, return value "2." Thus, smaller number means higher contact. Data were collected and analyzed using a personal computer and commercially available software (Time HC; O'Hara, Tokyo, Japan).

2.5.2. Motor coordination and motor learning test (rotarod)

Mice were individually placed on a rotating rod (O'Hara, Tokyo, Japan) and the time each animal was able to maintain its balance walking on top of the rod was measured. The speed of the rotarod was 4 rpm (on the first day) or accelerated from 4 to 40 rpm over a 4-min period and 40 rpm another 1 min (day 2 to day 5). Mice were given a trial for 2 min (day 1) or four trials with a maximum time of 300 s (inter-trial intervals were 20–30 s). Time between placement and falling or revolving around the rod was recorded manually.

2.5.3. Sucrose preference test

Mice were tested for a 3-days 24-h test and 1-day 1-h test with water deprivation. The 24-h tests were free choice between two bottles, one with sucrose (3% in filtered water) and another with filtered water. To eliminate the side preference, the position of bottles was switched every 24 h. The consumption of water and sucrose solution was assessed daily. After the choice test, mice were deprived water for 24 h and then a 1-h choice test between water and sucrose was conducted.

2.5.4. Tail suspension test

Mice were individually hung by the tail using an adhesive tape placed approximately 1.5 cm from the tip of the tail attached to a wire and 30 cm above the floor. The duration of immobility was scored and analyzed using Image J TS (O'Hara, Tokyo, Japan) for 5 min.

2.5.5. Forced swimming test

Mice were individually placed for 15 min (day 1) or 5 min (day 2) in glass cylinders (30 cm high, 10 cm in diameter) containing 10 cm of water maintained at 23–25 °C. The duration of immobility was scored and analyzed using Image J software. The immobility time during the first 5 min was assessed.

2.5.6. Marble burying test

The test was performed in the test cage identical to their home cage with a 5-cm thick layer of bedding material (TEK-FRESH, Edstrom Industries, Waterford, WI, USA). Mice were habituated to fresh bedding for 30 min and then briefly returned to their home cage; 20 glass marbles (1.5 cm in diameter) were placed evenly on the bedding. Mice were then reintroduced into the test cage and the number of buried marbles (buried into the bedding over 2/3) was analyzed 30 min later.

2.5.7. Hot plate and tail flick test

In the hot plate test (Model MK-350C, Muromachi-kikai, Tokyo, Japan), mice were individually placed on the plate (52 ± 0.5 °C) enclosed in a translucent plastic wall, and the time between placement and licking of the paws and jumping was recorded manually as the response latency. A cut-off time was 90 s. Because most of the mice did not jump, latency to licking was used for statistical analysis.

In the tail flick test (Model MK-330B, Muromachi-kikai, Tokyo, Japan), mice were individually restricted on the radiant heat meter and focused heat was applied to the surface of the tail at 2–3 cm from its tip; the latency to reflexive removal of the tail from the heat was recorded manually as the tail flick latency. A cut-off time was 10 s.

In these tests, data were obtained by two observers, and the shorter scores were adopted as the response time.

2.5.8. Statistical analysis

For statistical analysis of behavioral analyses phases I–III, the Student's *t*-test, one-way ANOVA, and repeated measures ANOVA (RMANOVA) were used. When a significant effect was found by one-way ANOVA, Tukey post hoc comparisons were applied. When sphericity was rejected by the Mauchly test before the application of RMANOVA, the Greenhouse-Geisser estimate was used. Paired *t*-test and two-sample *t*-test were also used for post hoc analysis when necessary. These statistical analyses were performed using SPSS 11.0 for Windows (SPSS Japan, Tokyo, Japan). Significance levels were set at 0.05 (two-tailed); d.f., degree of freedom. Average and standard error of mean (S.E.M.) were presented for each experimental parameter in one group.

2.6. Immunohistochemistry

Because several computer programs predicted that mouse *Wfs1* protein would be cleaved around position 36, we used the following amino acid sequence, Glu^{39}–Gly^{53} as an antigen. A hexadecapeptide (CEPPRAPRPQADPSAG) was synthesized, purified using high-performance liquid chromatography, and conjugated to keyhole limpet hemocyanin (KLH). Five Balb/c mice were injected intraperitoneally with the KLH-conjugated peptide emulsified in complete Freund's adjuvant. Antiserum was obtained 1 week after boosting with the same antigen. We performed Western blot analysis to selected sensitive antiserum specific to *Wfs1* protein.

For immunohistochemical analysis using *WfS1* antibody, wild-type B6 mice aged 20–22 weeks were used. The mouse brain was fixed by perfusion of paraformaldehyde and embedded with paraffin. Coronal or sagittal sections with the thickness of 8 μm were sliced from paraffin-embedded mouse brain.

After deparaffinization and hydration, the slices were incubated for 10 min at 95 °C in sodium citrate buffer. Endogenous peroxidase activity was quenched by H_2O_2/methanol treatment. For blocking, 0.8% Block Ace (Dainippon Sumitomo Pharma, Osaka, Japan) in phosphate-buffered saline (PBS) was used. Anti-*WfS1* antiserum was used by 2500× dilution. For second antibody, biotinylated anti-mouse IgG (Vector Laboratories, Burlingame, CA, USA) was used. Peroxidase/DAB staining was performed by Vectastain Elite ABC kit (Vector Laboratories).

2.7. DNA microarray analysis

DNA microarray analysis was performed in two developmental stages, 12 and 30 weeks old. Eight homozygous *Wfs1* KO mice and 8 WT littermates were sacrificed at the age of 12 weeks. Seven homozygous *Wfs1* KO mice and five WT littermates were also analyzed at the age of 30 weeks.

The hippocampus was rapidly dissected, and total RNA samples were extracted from the hippocampi using TRIzol reagent (Invitrogen, Carlsbad, CA, USA). Microarray analysis was performed according to the manufacturer's protocol (Affymetrix, Santa Clara, CA, USA). Briefly, 5 μg total RNA of each sample was reverse-transcribed into cDNA, and biotinylated cRNA was synthesized from the cDNA by in vitro transcription. DNA microarray experiments were performed using Mouse Genome 430 2.0 GeneChips (Affymetrix). The hybridization signal on the chip was scanned by a GeneArray scanner and processed by GeneSuite software (Affymetrix). The probe sets labeled as "present" in 8 of 16 samples at 12 weeks old (24703/45101 probe sets) or in 5 of 12 samples at 30 weeks old (24455/45101 probe sets) were selected. The raw data were analyzed using MAS5 (Affymetrix) and then imported into GeneSpring 7.3 software (Silicon Genetics, Redwood, CA). The signal intensity of each probe set on the microarray was divided by its median value using GeneSpring 7.3 software.

For statistical analysis, the Mann–Whitney *U*-test was performed between the KO mice and their WT littermates, and $P < 0.05$ was considered statistically significant.

The probe sets were classified based on the information from GeneOntology (http://www.geneontology.org/) using GeneSpring software. For the GeneOntology analysis, the differentially expressed probes were selected. The categories showing overrepresentation at the level of $P < 0.05$ and containing 10 or more probe sets were selected.

2.8. Real-time quantitative polymerase chain reaction (RT-PCR) analysis

The representative probe sets that showed altered expression in the DNA microarray analysis of mouse brains were verified by RT-PCR. The cDNA used for the DNA microarray analysis was used. Primers and probes for Gapdh, cde42ep5, Rnd1, Wnt2, and Garnl1 were commercially available by the Assay-on-Demand service (Applied Biosystems, Foster City, CA). The assays were carried out according to the protocols supplied by the manufacturer using 7900HT real-time PCR systems (Applied Biosystems). The relative values were calculated by measuring $\Delta C_t = C_t$ (each gene) $- C_t$ (Gapdh) for each sample in quadruplicate. For statistical analysis, one-tailed Mann–Whitney *U*-test was applied, and $P < 0.05$ was considered statistically significant.

3. Results

3.1. Wheel-running activity

To assess whether or not the *Wfs1* KO mice show bipolar disorder-like behavioral phenotypes, wheel-running activity of the *Wfs1* KO mice and WT littermates was recorded for a period up to 2 months. The levels of wheel-running activity and the circadian rhythm were assessed using male mice that were 34 weeks old at the initiation of this analysis (KO, $n = 11$; WT, $n = 9$). Average wheel-running activity per day of *Wfs1* KO mice during 28 days under the L-D condition did not differ from that of WT littermates (Fig. 1a; WT, 221.3 ± 64.7 [mean ± S.E.M.] counts; KO, 142.2 ± 57.6 counts, d.f. = 18, $U = 29$, $P = 0.21$ by Mann-Whitney *U*-test). Delayed activity

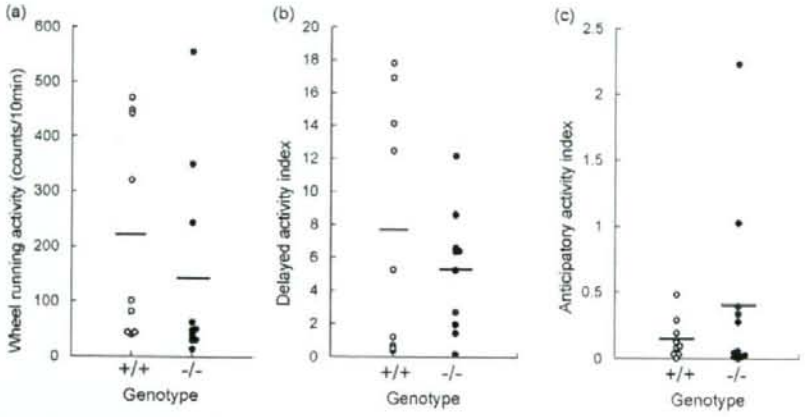

Fig. 1. Long-term wheel-running activity analysis. (a) Wheel-running activity. (b) Delayed activity index. Delayed activity index is defined as a percent of the wheel-running activity during the first 3 h of the light period with the total activity during the previous dark period (12 h). (c) Anticipatory activity index, the wheel-running activity in the last 3 h of light phase in comparison with the activity during dark phase. +/+, WT mice; −/−, *Wfs1* homozygous KO mice. Bars indicate averages. Each circle represents the datum of a mouse.

index (WT, 7.70 ± 2.50; KO, 5.29 ± 1.16, d.f. = 18, $U = 42$, $P = 0.84$) and anticipatory activity index (WT, 0.14 ± 0.05; KO, 0.34 ± 0.21, d.f. = 18, $U = 41$, $P = 0.78$) did not differ between the KO mice and WT littermates (Fig. 1a–c).

There was no abnormality of free running period measured at the constant dark condition in *Wfs1* KO mice (average 23.7 h, $n = 6$). None of female KO mice showed significant periodicity in wheel-running activity with the duration of 4–5 days (data not shown). These results show that the behavioral phenotypes of *Wfs1* KO mice are different from the mPolg Tg mice that exhibit altered circadian rhythm of wheel-running activity (Kasahara et al., 2006).

3.2. Behavioral analysis: phase I. Screening by a test battery

To screen the behavioral abnormality of *Wfs1* KO mice, we performed a conventional behavioral test battery using 14 homozygous KO mice, 14 heterozygous KO mice, and 13 WT littermates. The results of behavioral tests are summarized in Table 1.

3.2.1. Open-field test

Although a significant effect of time was found for both locomotor activity (d.f. = 8.6, $F = 3.0$, $P = 0.002$) and rearing (d.f. = 11.0, $F = 9.7$, $P = 0.000$), no significant effect of genotype was found for locomotor activity (d.f. = 2, $F = 0.70$, $P = 0.49$) and rearing (d.f. = 2, $F = 0.57$, $P = 0.56$). There was no significant interaction between time and genotype (locomotor, d.f. = 17.3, $F = 21.1$, $P = 0.57$; rearing, d.f. = 22.0, $F = 0.80$, $P = 0.71$) (Fig. 2a and b).

3.2.2. Startle response and prepulse inhibition

When RMANOVA was applied for the data of startle response, significant effect of blocks was found (d.f. = 5.12, $F = 7.80$, $P < 0.001$). However, no significant effect of genotype (d.f. = 2, $F = 0.664$, $P = 0.52$) or genotype × block block interaction (d.f. = 10.2, $F = 1.30$, $P = 0.22$) was found (Fig. 2c). No significant effect of genotype was found for the PPI ratio regardless of the interval of prepulse (50 ms, d.f. = 2, $F = 0.38$, $P = 0.68$; 100 ms, d.f. = 2, $F = 0.65$, $P = 0.52$; 200 ms, d.f. = 2, $F = 0.41$, $P = 0.66$, one-way ANOVA) (Fig. 2d).

3.2.3. Elevated plus maze

The number of entry into the open arms ($F = 0.31$, d.f. = 2, $P = 0.72$, one-way ANOVA) (Fig. 2e) and the time spent in the open arms ($F = 2.05$, d.f. = 2, $P = 0.14$) (Fig. 2f) were not significantly different among the genotypes. A significant effect of genotype was found for the total number of boluses ($F = 7.16$, d.f. = 2, $P = 0.002$) (Fig. 2g). The Tukey honest significant difference (HSD) test showed that homozygous KO mice had a significantly lower number of fecal boluses (2.7 ± 0.3 [mean ± S.E.M.]) compared with heterozygous KO mice (4.8 ± 0.5, $P = 0.01$) and WT mice (5.2 ± 0.5, $P = 0.004$).

Table 1
Summary of findings in behavioral tests

Test battery	Findings
Wheel-running activity (34 weeks, 11 KO, 9 WT)	
Periodicity	NS
Diurnal activity rhythm	NS
Phase I (12 weeks, 13 KO, 14 Hetero, 13 WT)	
Open field	NS
Startle/PPI	NS
Elevated plus maze	NS
Morris water maze	NS
Passive avoidance test	Longer latency to move
Active avoidance test	Reduced number of escape at day 3
Forced swimming test	Reduced immobility on the second day
Phase II (31 weeks, 9 KO, 11 WT)	
Home cage activity	NS
Open field	NS
Light-dark box	NS
Elevated plus maze	NS
Startle/PPI	NS
Morris water maze	Increased escape latency without the change of distance traveled
Fear conditioning	Enhanced freezing during conditioning and before the cue at the cue test
Phase III (9 weeks, 7 KO, 8 WT)	
Social interaction	Decreased interaction
Rota-rod	NS
Sucrose preference	NS
Tail suspension test	NS
Forced swimming test	Reduced immobility on the second day
Marble burying test	NS
Hot plate test	NS
Tail flick test	NS

KO, *Wfs1* (−/−); Hetero, *Wfs1* (−/+); WT, *Wfs1* (+/+). PPI: prepulse inhibition test, NS, non-significant.

3.2.4. Morris water maze

The time to reach the platform during the 5-day learning phase became shorter than the first day, shown by a significant effect of day by RMANOVA (d.f. = 4, $F = 19.1$, $P < 0.001$) (Fig. 2h). However, there was neither significant effect of genotype (d.f. = 2, $F = 0.56$, $P = 0.57$) nor significant interaction of day and genotype (d.f. = 2, $F = 0.53$, $P = 0.94$). The time spent in the target quadrant (d.f. = 2, $F = 0.10$, $P = 0.90$, one-way ANOVA) and immobility time (d.f. = 2, $F = 0.58$, $P = 0.56$) at the probe test performed on day 6 did not show a significant difference among the genotypes (Fig. 2i).

3.2.5. Passive avoidance test

The latency to escape at the conditioning phase was significantly different among the genotypes (d.f. = 2, $F = 4.70$, $P = 0.015$, one-way ANOVA). Multiple comparison showed that the latency in homozygous KO mice was significantly longer than that in WT mice ($P = 0.02$) (Fig. 3a). There was no significant difference in escape latency at the test session (d.f. = 2, $F = 0.81$, $P = 0.92$, one-way ANOVA).

3.2.6. Active avoidance test

The time course of mean escape latency was examined during 3-days' training, consisting of 5 blocks in each day

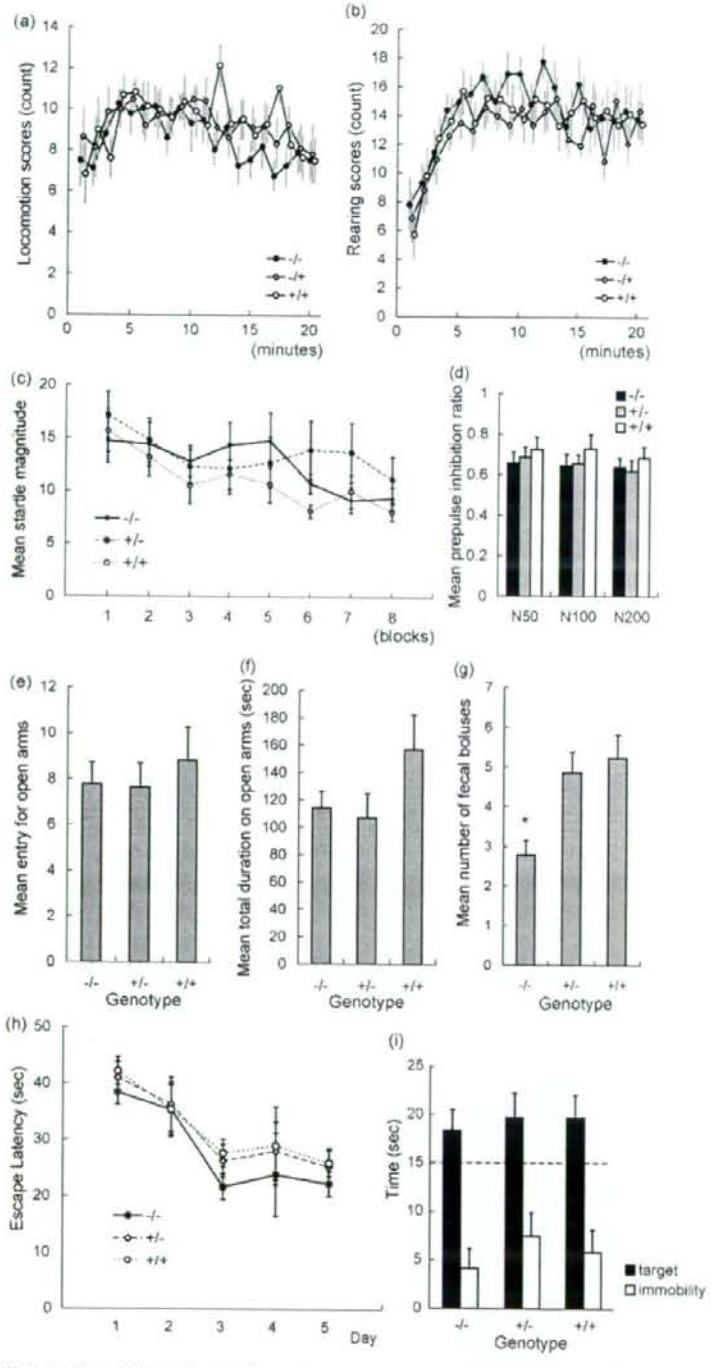

Fig. 2. Behavioral screening (1). (a–b) Open-field test. Locomotion scores (a) and rearing scores (b). Bars indicate the standard errors. (c) Startle response. (d) Prepulse inhibition test. N50 means the prepulse 50 ms before the startle pulse. (e–g) Elevated plus maze test. (h–i) Morris water maze test. Time course of escape latency during 5-days training (h), and time spent in the target quadrant during the 60-s session. Error bars represent standard error of mean. The dotted line represents the chance level. +/+, WT mice; +/−, *Wfs1* heterozygous KO mice; −/−, *Wfs1* homozygous KO mice. $^{*}P < 0.05$.

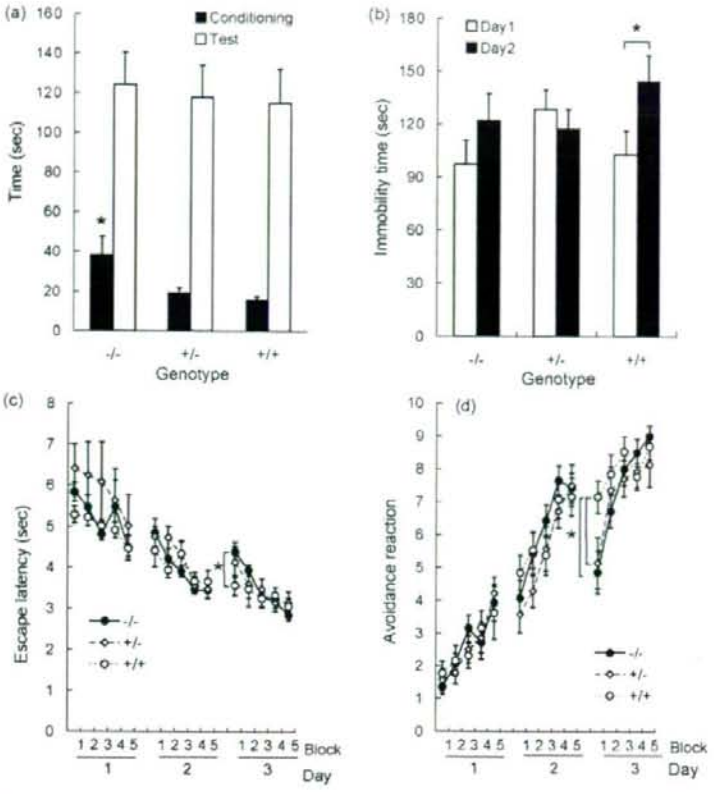

Fig. 3. Behavioral screening (2). (a) Passive avoidance test. (b) Forced swimming test performed on two sequential days. (c–d) Active avoidance test. +/+, WT mice; +/−, *Wfs1* heterozygous KO mice; −/−, *Wfs1* homozygous KO mice. Error bars represent standard error of mean. $^{*}P < 0.05$.

(Fig. 3c). In the three-way RMANOVA with the within-group factors of day and block and the between-group factor of genotype, although no significant effect of genotype was found (d.f. = 2, $F = 0.75$, $P = 0.47$), there was a significant interaction between genotype and block (d.f. = 1.75, $F = 2.94$, $P = 0.007$). No other two-way or three-way interactions were statistically significant. This significant interaction may be caused by longer escape latency of KO mice only at the first block. A post hoc analysis showed that the escape latency of the homozygous KO mice at the first block on day 3 was significantly longer than that in WT mice (d.f. = 25, $t = 2.34$, $P = 0.027$, with no correction for multiple comparison).

Similar interaction between genotype and block was also seen for the numbers of avoidance (d.f. = 6.3, $F = 3.25$, $P = 0.004$) (Fig. 3d). Both homozygous and heterozygous KO mice showed significantly lower numbers of avoidance at the first block on day 3 (homozygotes, d.f. = 25, $t = -2.82$, $P = 0.009$; heterozygotes, d.f. = 25, $t = -2.15$, $P = 0.04$).

3.2.7. Forced swimming test

When the immobility time was analyzed by RMANOVA, a significant effect of day (d.f. = 1, $F = 5.5$, $P = 0.024$) and a significant interaction of day and genotype (d.f. = 2, $F = 3.8$, $P = 0.031$) were found, whereas no significant effect of genotype was found (d.f. = 2, $F = 0.48$, $P = 0.61$) (Fig. 3b).

In the WT mice, immobility time was significantly longer on the second day (144.6 ± 53.0 s) compared with the first day (103.0 ± 48.3 s, d.f. = 12, $t = -3.45$, $P = 0.005$, paired *t*-test), possibly reflecting the learned despair (Parra et al., 1999). On the other hand, such a significant increase of immobility time on the second day was not observed for heterozygous (day 1, 128.5 ± 39.4 s; day 2, 117.5 ± 39.4 s; d.f. = 12, $t = 1.11$, $P = 0.28$) and homozygous (day 1, 97.4 ± 50.6 s; day 2, 122.0 ± 57.0 s; d.f. = 13, $t = -1.44$, $P = 0.17$) KO mice (Fig. 3b).

3.2.8. Summary of the phase I behavioral analysis

The results of the phase I behavioral analysis are summarized as follows.

(1) There was no abnormality in open field, elevated plus maze, PPI, and Morris water maze. However, it cannot be ruled out that the mice develop behavioral phenotypes at later age because depression is an adult-onset disease.
(2) The passive avoidance test showed the longer latency to enter the other chamber in *Wfs1* KO mice. This could be

explained either by low anxiety or retardation, that is slow movement or delayed onset of motion. However, it is also possible that mice could have been just busy exploring the first box, or they had some kind of place neophobia.

(3) The active avoidance test showed longer escape latency and lower numbers of avoidance at the first block on day 3 in *Wfs1* KO mice. This might suggest that the emotional memory is impaired in the *Wfs1* KO mice. It cannot be excluded, however, that *Wfs1* KO mice have impairment of pain sensitivity.

(4) Altered response to serial forced swimming test. This may suggest that the *Wfs1* KO mice tend to be resistant to behavioral despair.

3.3. Behavioral analysis: phase II

To further characterize the behavioral phenotypes of *Wfs1* KO mice, additional behavioral analysis was performed.

3.3.1. Open-field, elevated plus maze, PPI tests, and Morris Water Maze at 31 weeks

At first, four of behavioral tests were repeated in the mice aged 31 weeks to assess the effect of age. There were no significant difference between WT mice and *Wfs1* KO mice for three of these behavioral tests: open-field, elevated plus maze, and PPI tests (data not shown).

On the other hand, the Morris water maze test showed longer escape latency. Two-way RMANOVA showed significant effects of genotype (d.f. = 1, $F = 9.04$, $P = 0.008$) and day (d.f. = 3, $F = 8.45$, $P < 0.001$) (Fig. 4a). The *Wfs1* KO mice showed longer escape latency than controls. There was no significant interaction between genotype and day (d.f. = 3, $F = 0.60$, $P = 0.61$). On the other hand, there was no significant effect of genotype on the distance (d.f. = 1, $F = 0.38$, $P = 0.54$) (Supplementary Fig. 1a). Effect of day was significant (d.f. = 3, $F = 25.2$, $P < 0.001$), but the interaction between genotype and day was not significant (d.f. = 3, $F = 0.71$, $P = 0.54$). To assess the speed of swimming, a new index, swimming speed index = (total distance)/(latency to reach platform) was calculated. Two-way RMANOVA showed no significant effects of day (d.f. = 1.77, $F = 2.57$, $P = 0.09$) and genotype (d.f. = 1, $F = 0.04$, $P = 0.83$). There was no significant day × genotype interaction (d.f. = 1.77, $F = 0.33$, $P = 0.69$) (Supplementary Fig. 1b). Spatial memory cannot be assessed because no significant difference was found between the time spent in the target quadrant and that in the other three quadrants, suggesting that the probe test did not work properly even for wild-type mice (data not shown).

3.3.2. Home cage activity

To assess the general activity level, home cage activity was recorded for 8 days. When RMANOVA was applied, a significant effect of day (d.f. = 5, $F = 5.95$, $P < 0.001$) was found. There was no significant effect of genotype (d.f. = 1, $F = 0.61$, $P = 0.44$) and genotype × day interaction (d.f. = 5, $F = 0.53$, $P = 0.75$) (Fig. 4b).

3.3.3. Anxiety-like behavior

Next, the level of anxiety-like behavior was further assessed by the L-D box. The marble burying test was also performed in the 9-week-old mice in the phase III behavioral analysis.

In the L-D box test, no significant difference was found in the time spent in the light box (WT, 39.2 ± 9.0%, KO, 37.1 ± 9.8%, d.f. = 18, $t = 0.50$, $P = 0.61$). There was no significant difference in the number of marbles buried (WT 16.0 ± 0.8, KO 17.1 ± 0.7, $t = 1.0$, $P = 0.33$). These findings suggest that longer latency to escape at the passive avoidance test was not due to lower anxiety-like behavior.

3.3.4. Emotional memory

To test the hypothesis that emotional memory is impaired in the *Wfs1* KO mice, the fear conditioning test was performed.

During the conditioning phase, two-way RMANOVA revealed significant effect of genotype (d.f. = 1, $F = 4.47$, $P = 0.049$) and time (d.f. = 3.54, $F = 22.1$, $P < 0.001$). No significant period × genotype interaction was found (d.f. = 3.54, $F = 1.73$, $P = 0.16$). The *Wfs1* KO mice showed significantly longer time of freezing during the conditional stimuli (periods 5 and 7) and at the final period (Student's *t*-test, $P < 0.05$) (Fig. 4c).

For the cue test, two-way RMANOVA was applied to the data set before and after the cue, separately. For the data of freezing before the cue, a slight tendency of the effect of genotype (d.f. = 1, $F = 2.9$, $P = 0.10$) was seen, whereas there was significant effect of time (d.f. = 3, $F = 5.93$, $P = 0.001$) and no interaction between genotype and time (d.f. = 3, $F = 0.30$, $P = 0.82$). The *Wfs1* KO mice spent a significantly longer time for freezing ($t = 2.48$, $P < 0.01$) (Fig. 4d). However, no significant effect of genotype was found after the cue (effect of genotype, d.f. = 1, $F = 1.48$, $P = 0.23$; effect of time, d.f. = 3, $F = 1.60$, $P = 0.19$; genotype × time interaction, d.f. = 3, $F = 0.40$, $P = 0.75$). There was no significant effect of genotype at the context test (Fig. 4e).

These findings suggested that memory of emotion is not impaired in the *Wfs1* KO mice.

3.4. Behavioral analysis: phase III

3.4.1. Pain sensation

As noted above, it cannot be excluded that *Wfs1* KO mice have impairment of pain sensitivity. To rule out such possibility, the hot plate test and tail flick test were performed. No difference in the latency to licking (WT, 10.3 ± 1.2 s; KO, 9.9 ± 0.9 s, $t = 0.219$, d.f. = 12, $P = 0.83$, by Student's *t*-test) was found between the *Wfs1* KO mice and WT mice by the hot plate test. There was no significant difference in the latency to flick the tail (WT, 3.5 ± 0.2 s; KO, 3.4 ± 0.2 s, d.f. = 12, $t = 0.29$, $P = 0.77$).

3.4.2. Motor function

As noted above, many of the positive findings in behavioral tests can be interpreted as reflecting retardation. Such findings can be explained by altered motor functions, such as impairment in muscle contraction, voluntary movement, or

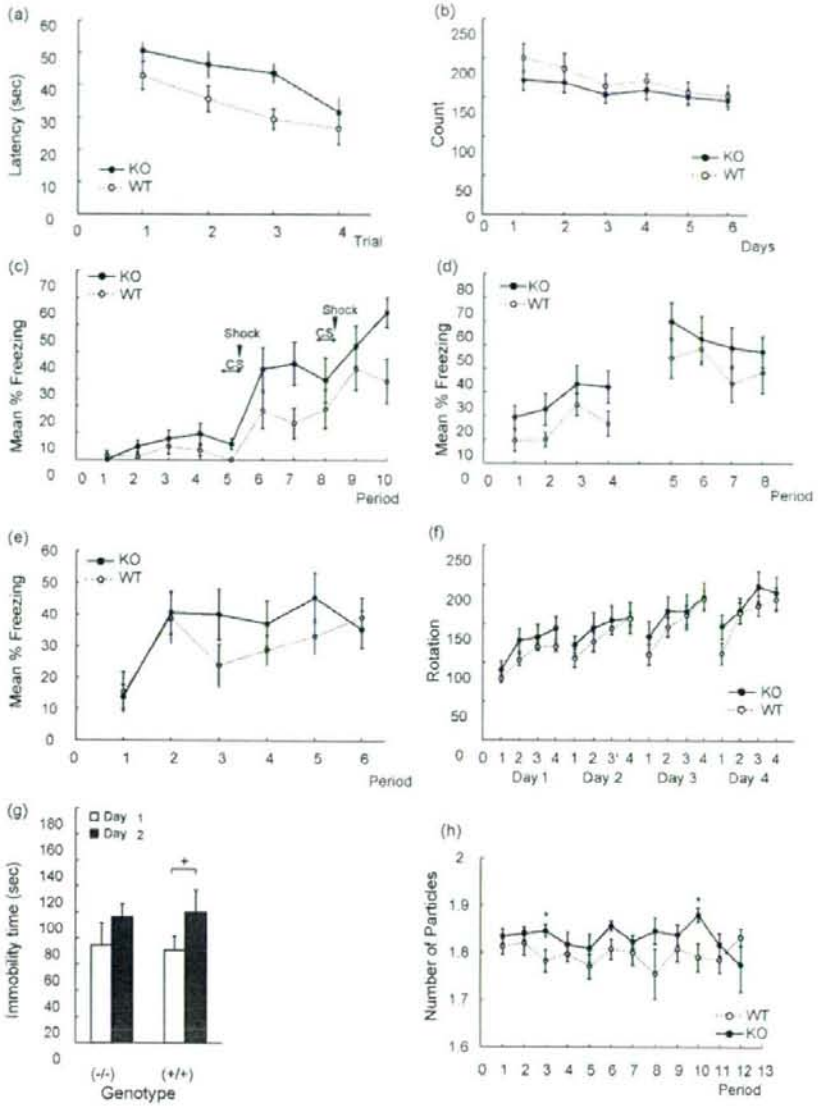

Fig. 4. Further characterization of behavioral phenotypes of *Wfs1* KO mice. (a) Morris water maze test. (b) Home cage activity. (c and d) Fear conditioning test. One time period is 30 s. (c) Conditioning phase. Conditional stimuli (tone) and unconditional stimuli (foot shock) were applied during periods 5 and 8. (d) Cue test. Cue was applied between the time periods 4 and 5. (e) Context test. (f) Rotarod test. (g) Forced swimming test. (h) Social interaction test. Note that high number of particles indicates lower levels of social interaction.

motor coordination. To test this possibility, the rotarod test was performed. Three-way RMANOVA with the intra-individual factors of day and trial and inter-individual factor of genotype showed no significant effect of genotype (d.f. = 1, $F = 1.02$, $P = 0.33$). Whereas significant effects of day (d.f. = 3, $F = 15.6$, $P < 0.001$) and trial (d.f. = 3, $F = 51.0$, $P < 0.001$) were found, no significant two-way or three-way interactions were detected except for a trend of interaction between day and trial (d.f. = 3, $F = 2.54$, $P = 0.07$) (Fig. 4f).

3.4.3. Behavioral despair

As noted above, *Wfs1* KO mice showed altered response to the serial forced swimming test. To further confirm this finding, the forced swimming test was performed again.

RMANOVA revealed a tendency of effect of day (d.f. = 1.0, $F = 3.83$, $P = 0.07$). There was no significant effect of genotype (d.f. = 1, $F = 0.18$, $P = 0.67$) and day × genotype interaction (d.f. = 1.0, $F = 0.17$, $P = 0.68$).

Although no day × genotype interaction was found in this analysis, the paired *t*-test was applied similarly to the first experiment (Fig. 4g). Immobility time tended to be longer on the second day (99.7 ± 17.4 s) compared with the first day (71.0 ± 10.55 s, $r = 0.68$, $P = 0.064$, paired *t*-test) in WT mice, whereas no significant difference was found in *Wfs1* KO mice (day 1, 74.5 ± 17.1 s; day 2, 96.2 ± 10.0 s, $r = 0.50$, $P = 0.24$). This analysis showed a similar tendency to the first experiment.

The other test of behavioral despair, the tail suspension test, was also performed. There was no significant difference in the immobile time between the *Wfs1* KO mice and WT mice (WT, 9.0 ± 2.8%; KO, 9.4 ± 3.0%, $t = 0.09$, $P = 0.92$).

3.4.4. Other aspects of depression

Some of these noted findings in the *Wfs1* KO mice can be explained by the retardation in emotionally triggered motion. This could not be explained by abnormalities in instrumental motor functions. Such findings seem to be similar to "psychomotor retardation" seen in human depressive patients. Though the findings in the forced swimming test and tail suspension test are equivocal, behavioral despair is not always a valid depression model. Thus, we further examined the other aspects of depression.

The sucrose preference test is an established test for anhedonia, one of the core symptoms of depression. In the choice test for 3 days, there was no significant effect of genotype (d.f. = 1, $F = 0.95$, $P = 0.34$) by two-way RMANOVA (WT, day 1, 44.2 ± 16.7%, day 2, 94.1 ± 5.2%, day 3, 84.5 ± 9.7%; KO, day 1, 37.3 ± 12.9%, day 2, 97.3 ± 1.7%, day 3, 60.2 ± 16.0%). A significant effect of trial (d.f. = 2, $F = 10.7$, $P = 0.001$) and no significant interaction of genotype × trial was found (d.f. = 2, $F = 0.68$, $P = 0.51$). The 1-h choice test after 24-h water deprivation did not show a significant difference between genotypes (WT 90.2 ± 1.7%, KO 86.3 ± 5.3%, $U = 28$, NS).

The social interaction test is an established test for anxiety-like behavior (File and Seth, 2003). However, its response to drugs is different from elevated plus maze, and it is more sensitive to serotonergic drugs. Recently, this test is also applied to animal models of schizophrenia (Miyakawa et al., 2003) and autism, and to genetic models of anxiety and depression (Overstreet et al., 2003). Thus, social behavior of the *Wfs1* KO mice was examined by this test. Two-way RMANOVA revealed no significant effect of genotype (d.f. = 1, $F = 2.0$, $P = 0.17$) and time (d.f. = 11, $F = 0.93$, $P = 0.51$). There was a trend of genotype × time interaction (d.f. = 11, $F = 1.67$, $P = 0.08$) (Fig. 4h). The *Wfs1* KO mice showed significant decrease of social interaction at the periods 3 and 10 (Student's *t*-test, $P < 0.05$) shown by the higher number of particles observed.

3.5. Wfs1 immunohistochemistry

To determine the molecular basis of behavioral abnormality in *Wfs1* KO mice, we verified whether the distribution of *Wfs1* protein in the brains of WT B6 mice is similar to that in rats (Fig. 5a–f) (Takeda et al., 2001). We verified that no staining was observed in *Wfs1* KO mice, suggesting the specificity of the anti-*Wfs1* antibody (Fig. 5g).

Wfs1-like immunoreactivity (*Wfs1*-IR) localized mostly to neurons and its regional distribution was mostly similar to that in rats (Fig. 5a). *Wfs1*-IR was most abundant in the hippocampal CA1 pyramidal neurons (Fig. 5b), and strong in the layer II pyramidal neurons of the cerebral cortex (Fig. 5c). Similar to rats, *Wsf1*-IR was also rich in the striatum, nucleus accumbens, thalamus, cerebellar Purkinje cells, amygdala, and bed nucleus of the stria terminalis (Fig. 5d). In addition, *Wfs1*-IR was observed in several hypothalamic nuclei, such as the paraventricular nucleus and suprachiasmatic nucleus (SCN) in mice (Fig. 5e). In the adjacent region of SCN, sub-paraventricular zone, some cell bodies showed *Wfs1*-IR. The ventromedial nucleus and arcuate nucleus also showed *Wfs1*-IR (Fig. 5f). *Wfs1*-IR was also found in the locus coeruleus and cochlea nucleus (data not shown).

3.6. DNA microarray analysis

To examine what sort of functional impairment occurs in the neurons of *Wfs1* KO mice, we performed gene expression analysis using DNA microarray. Because *Wfs1*-IR was most abundant in hippocampus, we performed DNA microarray analysis in the hippocampus of the *Wfs1* KO mice. A total of 1012 probe sets were changed at the age of 12 weeks. To narrow down the gene list, we repeated the experiment at the age of 30 weeks. We assumed that the true gene expression difference observed at age 12 weeks should be replicated at age 30 weeks. At the age of 30 weeks, 3508 probe sets showed significant differences. The genes altered in the same direction at both the ages of 12 and 30 weeks, and the fold change higher than 1.2 are shown in Table 2.

GeneOntology (GO) analysis showed that genes related to ribosome biogenesis (GO:3735: structural constituent of ribosome, GO:7046: ribosome biogenesis, GO:3723: RNA binding) or other basic cellular functions (GO:5622: intracellular, GO:44249: cellular biosynthesis, GO:15399: primary active transporter activity, GO:5623: cell, GO:7028: cytoplasm organization and biogenesis) were commonly up-regulated at the age of 12 and 30 weeks (Supplementary Tables 1 and 2). The major difference between the weeks 12 and 30 is the inclusion of neurodevelopment-related genes at the age of 30 weeks (GO:48666: neuron development, GO:30182: neuron differentiation, GO:7409: axonogenesis, GO:48667: neuron morphogenesis during differentiation, and GO:31175: neurite morphogenesis) (Supplementary Table 2).

3.7. RT-PCR analysis

To test whether the findings by DNA microarray analysis are chance findings, RT-PCR analysis was performed. For this purpose, two down-regulated genes, *cdc42ep5* and *Rnd1*, as well as two up-regulated genes, *Wnt2* and *Garnl1*, were examined using Gapdh as a reference.

The level of cdc42ep5 and Rnd1 tended to be lower at 12 weeks but not at 32 weeks. On the other hand, Wnt2 and Garnl1

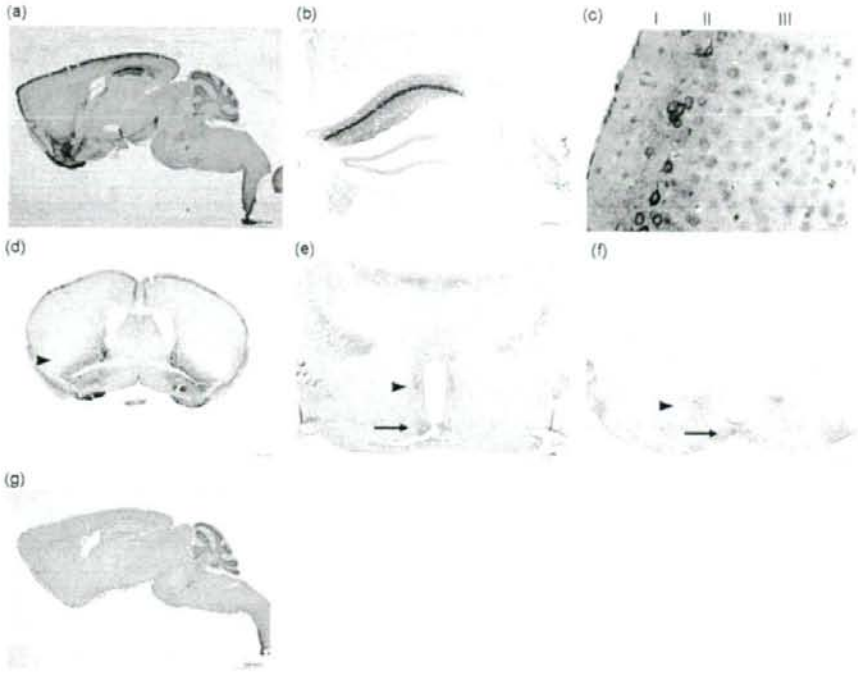

Fig. 5. Localization of *Wfs1*-like immunoreactivity in mouse brain. Immunohistochemistry analysis of mouse brain using anti-*Wfs1* antiserum. Coronal sections are shown except for panel a. (a) Sagittal section of the whole brain. (b) Hippocampus. CA1 (corpus ammon 1) region is selectively stained. (c) Cerebral cortex. Layer II pyramidal neurons are stained. (d) Coronal section at the level of bed nucleus of striata terminalis (BNST). At this level, the regions with intense *Wfs1*-IR looked as if they are surrounding the internal capsule (arrowhead). (e and f) Hypothalamus. Suprachiasmatic nucleus and sub-paraventricular zone are indicated by an arrow and an arrowhead, respectively (e). Arcuate nucleus and ventromedial nucleus are shown by an arrow and an arrowhead, respectively (f). (g) Immunohistochemistry analysis of the brain of a *Wfs1* KO mouse using anti-*Wfs1* antiserum. No staining is detected.

were significantly up-regulated at 32 weeks but not at 12 weeks (Table 3).

4. Discussion

4.1. Behavioral analyses

We recently reported that mPolg Tg mice show bipolar disorder-like behavioral phenotypes, such as altered circadian rhythm in both males and females and periodic fluctuation of wheel-running activity in females (Kasahara et al., 2006). Based on previous reports suggesting that patients with Wolfram disease are frequently affected with depression or bipolar disorder, we speculated that the *Wfs1* KO mice might also show these bipolar disorder-like phenotypes, which were seen in the mPolg Tg mice. However, *Wfs1* KO mice did not show similar phenotypes (Fig. 1).

Thus, we next examined the possibility that *Wfs1* KO mice show other types of behavioral phenotypes. At first, a battery of established behavioral tests was applied. There was no marked difference found in most of conventional behavioral tests, such as the open-field test, startle response, prepulse inhibition test, and elevated plus maze. The lack of marked difference in these tests was replicated in the mice aged 31 weeks. On the other hand, several tests in the initial test battery showed equivocal findings. In the passive avoidance test, the mice showed longer latency to move into the dark compartment at the training phase (Fig. 3a). The active avoidance test showed subtle differences between the KO and WT mice. On the third day of training, WT mice kept the same level of escape latency and number of avoidance reactions as the final block of the second day. Although, *Wfs1* KO mice seemed as if they forget the previous memory of escape training (Fig. 3c and d), it is unlikely considering the fact that there were no differences in the day 2 of the active avoidance test and in the contextual testing of the fear conditioning test. Otherwise, they may remember the events, but could not take the adequate action under the situation for some other reasons. For example, a possibility is that they showed retardation or increased behavioral despair without any problems in memory retention. In the forced swimming test performed for two sequential days, WT mice showed an increase of immobility time on the second day (Fig. 3d). This is in accordance with a previous study showing that mice became immobile on the second day of the sequential forced swimming test (Parra et al., 1999). This phenomenon was not observed in the homozygous and heterozygous KO mice (Fig. 3d). Although statistical analysis did not show the same difference, a similar tendency was observed in the second

Table 2
Probe sets commonly altered both at 12 and 30 weeks

Probe set ID	*P*-value		Fold change		Gene symbol	chromosome	Gene title
	12W	30W	12W	30W			
Down							
1433815 at	0.0008	0.0074	−2.24	−1.72	Jakmip1	5qB3[a]	Janus kinase and microtubule interacting protein 1
1448411 at	0.0008	0.0045	−2.10	−2.00	*Wfs1*	5qB3[a]	Wolfram syndrome 1
1419744 at	0.0357	0.0424	−1.45	−1.44	H2-DMb2	17qB1	Histocompatibility 2, class II, locus Mb2
1442241 at	0.0357	0.0424	−1.41	−1.49	Srpk2	5qA3[a]	Serine/arginine-rich protein specific kinase 2
1425620 at	0.0157	0.0284	−1.39	−1.22	Tgfbr3	5qE5[a]	Transforming growth factor, beta receptor III
1418712 at	0.0274	0.0284	−1.36	−1.47	Cdc42ep5	7qA1	CDC42 effector protein (Rho GTPase binding) 5
1441317 x at	0.0011	0.0045	−1.34	−1.71	Jakmip1	5qB3[a]	Janus kinase and microtubule interacting protein 1
1455197 at	0.0357	0.0424	−1.26	−1.29	Rnd1	15qF1	Rho family GTPase 1
Up							
1418148 at	0.0087	0.0074	2.03	1.68	Abhd1	5qB1[a]	Abhydrolase domain containing 1
1431328 at	0.0046	0.0424	1.50	1.21	Ppp1cb	5qB1[a]	Protein phosphatase 1, catalytic subunit, beta isoform
1459714 at	0.0157	0.0284	1.35	1.57	–	4qE1	–
1449425 at	0.0357	0.0074	1.28	1.28	Wnt2	6qA2	Wingless-related MMTV integration site 2
1457532 at	0.0357	0.0185	1.27	1.35	Garnli	12qC1	GTPase activating RANGAP domain-like 1
1416569 at	0.0274	0.0118	1.25	1.24	Actl6a	3qA3	Actin-like 6A
1446406 at	0.0460	0.0424	1.24	1.20	Paqr8	1qA4	Progestin and adipoQ receptor family member VIII
1446815 at	0.0357	0.0424	1.23	1.29	Dph4	2qE3	DPH4 homolog (JJJ3, S. cerevisiae)
1456328 at	0.0460	0.0284	1.22	1.33	Bank1	3qG3	B-cell scaffold protein with ankyrin repeats 1

[a]The probe sets on the chromosome 5.

forced swimming test. In addition, the other test for behavioral despair, the tail suspension test, did not show any significant difference. On the other hand, the longer escape latency of the KO mice without the difference of the distance traveled in the Morris water maze might reflect the longer time for immobility during the session. Thus, the *Wfs1* KO mice might show enhanced or attenuated behavioral despair depending on experimental conditions.

Table 3
Validation study of gene expression using RT-PCR

Gene	Genotype	N	Average	S.E.M.	*P*-value
12w					
cdc42ep5	WT	8	0.68	0.02	
	KO	8	0.63	0.02	0.088*
Rnd1	WT	8	0.42	0.01	
	KO	8	0.39	0.02	0.070*
Wnt2	WT	8	0.42	0.01	
	KO	8	0.44	0.02	0.227
Garnl1	WT	8	15.30	0.37	
	KO	8	14.62	0.61	0.180
32w					
cdc42ep5	WT	5	0.63	0.01	
	KO	7	0.66	0.03	0.225
Rnd1	WT	5	0.58	0.04	
	KO	7	0.54	0.04	0.235
Wnt2	WT	5	0.40	0.01	
	KO	7	0.44	0.02	0.041**
Garnl1	WT	5	12.95	0.16	
	KO	7	14.37	0.64	0.049**

The gene expression levels were normalized by Gapdh. Each value represents the gene/Gapdh ratio $\times 10^{-2}$. *P*-values were calculated by Mann–Whitney *U*-test (one tailed).
* $P < 0.10$
** $P < 0.05$.

As described above, it was speculated that longer latency to move at the passive avoidance test can be explained either by low anxiety or retardation of *Wfs1* KO mice. The former possibility was not supported by two established tests for anxiety-like behavior, the L-D box test, and the marble burying test.

Wfs1 KO mice also showed longer escape latency and lower numbers of avoidance during the active avoidance test. This was not due to decreased pain sensitivity. This cannot be explained by the impairment of emotional memory, because there was no significant abnormality in fear conditioning test. This test instead showed increased freezing during conditioning phase. Freezing was also increased during the cue test, not after the cue but before the cue.

The *Wfs1* KO mice did not show impairment in fundamental motor functions that can explain these findings.

In summary, the following findings were obtained.

(1) Longer latency to move in passive avoidance test.
(2) Diminished avoidance reaction during active avoidance test.
(3) Longer escape latency in Morris water maze.
(4) Increased freezing during conditioning.
(5) Normal sensorimotor function and anxiety-like behavior.

These findings together suggest that the *Wfs1* KO mice might show retardation in the emotionally triggered motion. We could not discriminate whether this feature of the *Wfs1* KO mice reflects the slow movement, longer time to initiate movement, or mixture of both. Psychomotor retardation, that is, slow voluntary movement and thoughts and/or taking longer